

COCOSYS 3.1

Short Description



COCOSYS 3.1

Short Description

H. Wolff
N. Reinke
C. Spengler

June 2022
Revision 3

Imprint

Editor: Gesellschaft für Anlagen- und Reaktorsicherheit (GRS) gGmbH
Schwertnergasse 1
50667 Cologne

NOTICE

The code documentation is associated with the COCOSYS computer code. All sections of this documentation, like COCOSYS itself, are protected as intellectual property of GRS. Any duplication or distribution, if complete or in parts, is subject to the prior and express consent of GRS. Statements made within the documentation may be altered by GRS at any time.

The use of COCOSYS is licensed subject to the provisions of a Software Licence Agreement.

Acknowledgement:

The development of COCOSYS and the associated documentation are funded by the Federal Ministry for Economic Affairs and Energy (BMWi), currently under contract RS1561 and RS1579.

Table of contents

1	Short description of COCOSYS.....	1
1.1	Thermal Hydraulics	2
1.2	Simulation of aerosols, fission products and iodine.....	5
1.3	Behaviour of corium and concrete	7
2	Status of validation, plant applications	9
2.1	Examples of validation	11
2.1.1	THAI TH-13.....	11
2.1.2	EREC SLB-G02	15
2.1.3	BMC VANAM-M3	18
2.1.4	THAI Iod-11	22
2.1.5	MOCKA 5.7	26
2.2	Examples of plant application	30
2.2.1	Konvoi NPP.....	30
2.2.2	VVER-1000 NPP.....	34
3	References.....	38

1 Short description of COCOSYS

COCOSYS (CONtainment CODE SYStem) is a lumped-parameter code system for the comprehensive simulation of all relevant physical-chemical phenomena processes during design basis as well as severe accidents in containments of light water reactors.

The simulation of those phenomena and processes in the containment* of an NPP is required for the analysis of the potential consequences of accidents, and possible counter measures under conditions as realistic as possible. Therefore, at GRS the containment code system COCOSYS, a part of the GRS code package AC², based on mechanistic models has been developed /ARN 19/.

Mechanistic models are used as far as possible and reasonable for analysing the processes in containments. Essential interactions between individual processes, like e.g. between thermal hydraulics, hydrogen combustion as well as fission product and aerosol behaviour are treated in an extensive way. With such a detailed approach, COCOSYS is not restricted to relevant individual severe accident phenomena but also allows to demonstrate the interactions between these phenomena and the overall behaviour of the containment. The general structure of COCOSYS implemented in the code package AC² is shown in Fig. 1.1.

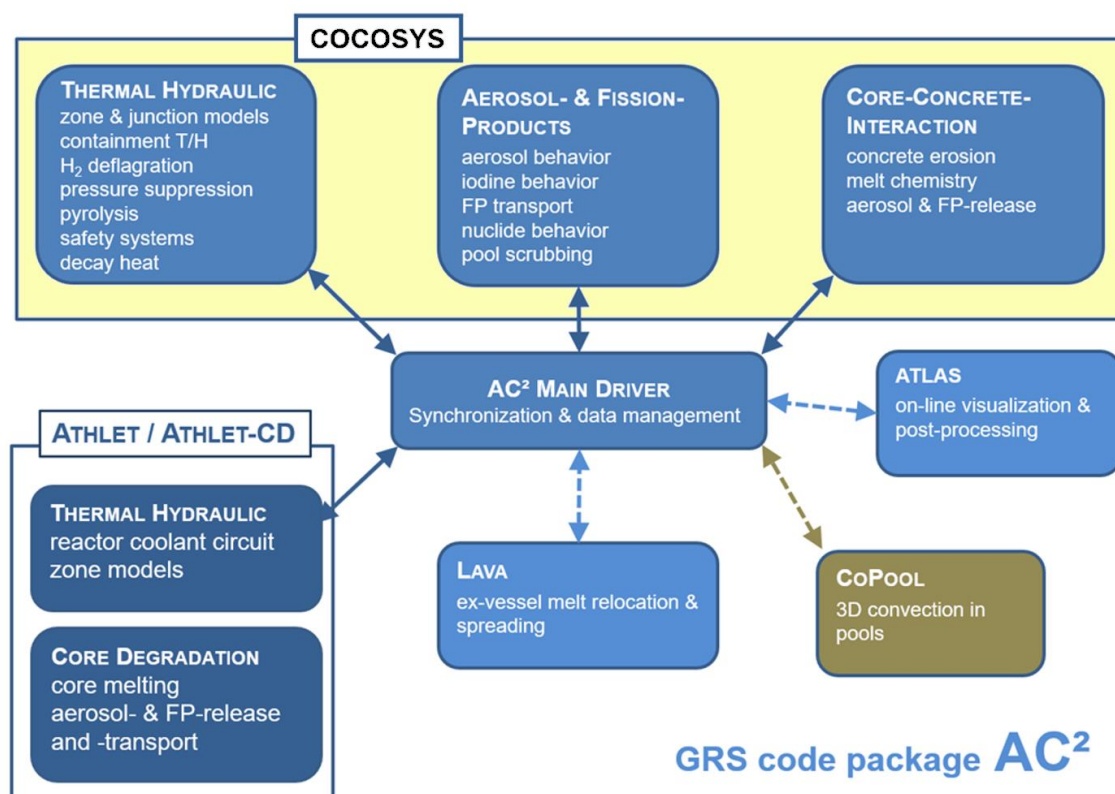


Fig. 1.1 Structure of COCOSYS 3.1 as part of AC²

* In the code description, the term "containment" includes also systems of hermetic compartments as they are constructed in nuclear power plants (NPP) with VVER-440 type reactors.

The COCOSYS code system consists of three main modules:

- **THY** for thermal hydraulics,
- **AFP** for the simulation of aerosols, fission products and iodine behaviour and
- **CCI** for corium and concrete behaviour.

Each module is a separately executable program, dedicated to one specific area or topic of the overall problem. Communication among these main modules is realised via a Message Passing Interface library (MPI /INT 20/). The AC² Main Driver organises and controls the calculation sequence. Each module calculates a part of the overall problem in such a way that they can be coupled at timestep level. Subsequently, the number of parameters that have to be exchanged is limited.

Apart from the main modules THY, AFP and CCI which belong to the kernel of COCOSYS, further programs provide for detailed simulation of specific phenomena, e.g. the inhouse-developed LAVA code for the simulation of spreading and dislocation of the melt /SPE 01/ or the CoPool code for the 3D simulation of thermal stratification in large water pools /ZEM 19/.

The overall coupling concept in COCOSYS is implemented in such a way that different modules can run in parallel. Furthermore, different coupling variants (calculation of the width of the synchronisation intervals, data exchange) can be predefined by the COCOSYS user. The data can be visualised both online (i.e. during the calculation) and offline (after termination of the calculation) by means of the ATLAS program. By coupling ATHLET/ATHLET-CD for reactor coolant circuit and core degradation processes and COCOSYS for containment ones, accident calculations can be performed for the complete plant.

1.1 Thermal Hydraulics

In COCOSYS, thermal hydraulic phenomena and processes in the containment are simulated in the main module **THY** using the lumped-parameter approach. The compartments of the considered containment of NPPs or test facilities have to be assigned to zones, whereas a compartment can be subdivided and represented by several zones. The thermodynamic state of a zone is defined by its temperature(s), pressure and masses of the specified components. For each defined zone energy and mass balance equations are solved. Zones can be split into several zone parts. All zone related variables are based on this structure (components, zone parts, zones, Fig. 1.2). To realize more complex boundary conditions or processes, a flexible program and data structure is realised. All dimensions are defined by dynamically allocated parameter statements.

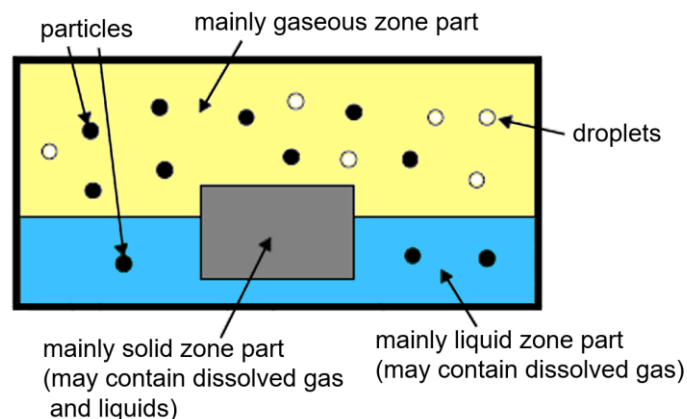


Fig. 1.2 General concept of zones in COCOSYS

The network concept (of differential equations) of the THY main module is written very general. It uses the integration package FTRIX/FEBE /LUT 96/ which is an implicit Euler forward Euler backward integration solver applied in the AC² code package. Using special system routines, it is relatively simple to introduce equations for new models.

Five **zone models** are implemented in COCOSYS:

- **Equilibrium zone model**

All components (liquid water, vapour and non-condensable gases) are assumed to be mixed homogeneously, resulting in a homogeneous distributed temperature in the zone (i.e. only one value). Superheated as well as saturated conditions are considered. Superheated atmospheres cannot contain liquid water. In these cases, the water is drained immediately into other zones. Using the concept of sump zones, a quasi non-equilibrium behaviour can be simulated. The application of the equilibrium zone model may be necessary in special cases, e.g. if water carry over has to be simulated for conservative design calculations.

- **Non-equilibrium zone model**

This model is the recommended standard zone model. Using this model, the zone is subdivided into two parts: the atmosphere part similar to the equilibrium zone model and a sump part (if existing) specified by its own temperature and water mass. At the water-atmosphere interface between both parts, heat exchange by convection and condensation (or evaporation/boiling) correlations is possible. In case of a coupled THY-AFP simulation the deposition rates of fog droplets are based on the AFP calculation.

- **Pressure suppression zone model DRASYS**

For the detailed simulation of short-term dynamic processes in pressure suppression systems, the DRASYS zone model was developed. The zone is subdivided into three zone parts: gas volume of the pipe, water pool and gas volume above the pool (Fig. 1.3).

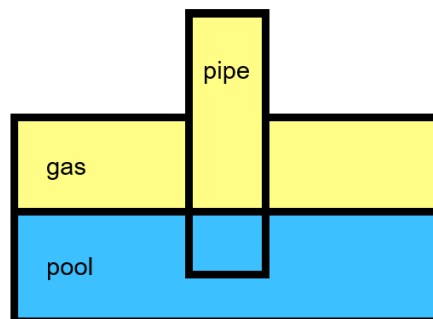


Fig. 1.3 General layout of the DRASYS zone model

- **Jet Vortex Condenser model VORTEX**

The VORTEX zone model is designed for the description of dynamic processes in a jet vortex condenser installed in selected NPPs with VVER-440/230 reactor. This specific zone model is subdivided into four zone parts: water pool, downcomer, vortex chamber including gas volume of the recirculation tank, and water volume in the recirculation tank.

- **Interface zone model**

This kind of zone model has to be used for the coupling of COCOSYS with a CFD code. The thermodynamic state variables needed are delivered by the connected CFD code. As described in the general zone concept, the zone may be subdivided into several zone parts.

In COCOSYS, a variety of **junction models** describes the flow between connected zones. The simulation of gas flow and water drainage is strongly separated, although water can be

transported via atmospheric junctions by gas flow (carried water droplets/fog, but no water deposited on floor) and dissolved gases can be transported via drain junctions. For an adequate simulation of the different systems or boundary conditions, specific junction models are implemented, like rupture discs, atmospheric valves, flaps/doors and specific pressure relief valves used in VVER-type reactors. For atmospheric junctions three flow types can be applied. They are based on the equations for incompressible, transient momentum flow as standard type, the incompressible, steady state momentum flow, and the compressible orifice flow. For the simulation of water drainage between zones, several models are realised, describing the sump balance using weir equation, water flow through openings in the zone bottom and drainage along walls considering the interaction between water flow and target structure surface. By means of the pump system model it is possible to simulate complete cooling systems, e.g. spray and emergency core cooling systems. To simulate any complete flooding of non-equilibrium-type zones with water, a special junction type is provided to calculate a flow composed of gas and water through single junctions between neighboured zones.

Walls, floors and ceilings of the considered containment compartments as well as installations are represented by metallic and/or non-metallic **structure objects** (heat slabs). These structures can be simulated as heat sinks/sources within zones and between them. The heat flux calculation is one-dimensional, solving the Fourier equation. Plate-type and cylinder-type structures can be modelled. The whole structure must be subdivided into layers. Their thermodynamic state is defined by a layer temperature. The arrangement of layers can be chosen freely. Modelling of gaps inside a structure is possible. The heat exchange between structures and their assigned zones is calculated via convection, condensation or radiation (including wall-to-wall) heat transfer correlations. In these correlations, averaged properties of the specified components are used. The initial temperature profile and the boundary conditions to the zones can be directly defined by the user.

For the simulation of severe accident sequences and possible accident management measures the simulation of **safety systems** is possible and **hydrogen related phenomena** are addressed. In THY one can model pump and spray systems, different types of coolers up to complete atmosphere cooling systems, ventilation systems, and ice condensers. Hydrogen recombination can be simulated by thermal recombiners as well as by passive autocatalytic recombiners (PARs). A special one-dimensional model was developed for box-type PARs (Fig. 1.4). Along the flow path a PAR can be subdivided into several segments. Each segment may contain a structure between the inner gas segment volume and the surrounding zone volume or inner structure elements. Using a diffusion-controlled reaction kinetics, the hydrogen recombination and, subsequently, the temperature profile inside the box of the catalytic plats and in the casing are calculated. Alternatively, simple correlations for mass conversion and assigned energy release are available for FR90 type PARs (AREVA vendor equation or GRS model). PAR types from other vendors, like AECL (Canada), NIS (Germany) or RVK (Russia) can be modelled as well. The recombination of CO is considered too.

The model FRONT was developed and implemented to simulate **hydrogen combustion** and flame propagation between different compartments without requiring much additional user input (e.g. additional combustion-specific nodalisation). It was validated against several hydrogen combustion experiments covering a broad spectrum of possible scenarios. The calculated combustion rates of hydrogen and deflagration velocities in the respective zones depend on several empirical correlations which include empirical parameters, what limits the predictive capabilities of the model for plant applications.

The THY module provides a model for the simplified **simulation of oil and cable fires**.

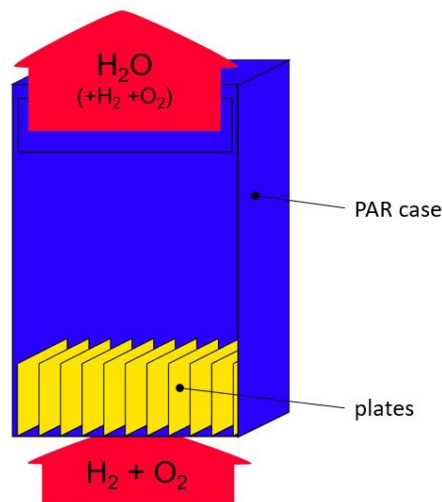


Fig. 1.4 Principal scheme of the hydrogen recombination model for plate type PAR in COCOSYS

1.2 Simulation of aerosols, fission products and iodine

The COCOSYS main module **AFP** is being developed for best-estimate simulations of the aerosol, fission product and iodine behaviour in the containment of LWRs. Both the THY and the AFP main modules consider the interactions between the thermal hydraulics and aerosol, fission product and iodine behaviour. There is a distinction in COCOSYS in the simulation of aerosol particles, radioactive fission products and the iodine chemistry, i.e. they are simulated by different models.

In the AFP main module of COCOSYS, the aerosol behaviour model is largely based on the AERIKA code. It treats up to eight chemically different aerosol components calculated with consideration of the thermal hydraulic boundary conditions. The module differentiates between soluble and insoluble as well as hygroscopic and non-hygroscopic aerosols. In the aerosol behaviour model, the mass of airborne aerosols and aerosols deposited on surfaces are considered. The following deposition processes are covered: sedimentation, diffusive deposition, thermophoresis and diffusio-phoresis on ceilings, side walls and floors. For the calculation of the condensation on the aerosols, the moving-grid method MGA is applied which reduces the numeric diffusion between the size categories considerably. In the case of hygroscopic aerosols, condensation may already occur under superheated conditions and can change the level of humidity in the atmosphere. This repercussion on the state of saturation is considered in the thermal hydraulic calculation as the aerosol behaviour close to saturation depends highly on the degree of saturation. There are special models for the simulation of HEPA fibre and granulate filters implemented in COCOSYS. They also consider the increasing pressure loss in the atmospheric junctions in the THY.

Furthermore, **SPARC-B/98** /FIS 98/ is part of the AFP module. It calculates the retention of aerosols during the transport of gas/steam mixtures through water pools and, finally, determines decontamination factors for the aerosols. These decontamination factors are used to calculate the deposition of aerosols in water pools. Among others, SPARC-B/98 is applied for the simulation of "pool scrubbing" in the pressure suppression system of boiling water reactors.

The **FIPHOST** module /ARN 98/ calculates the transport of the fission products within the containment. The fission products are treated as the radioactive part of the aerosol particles and the

radioactive non-condensable gases. FIPHOST differentiates between the atmosphere, the aerosol and the sump water as fission product carriers (see Fig. 1.5). Different to AERIKA, the fission products can be deposited on surfaces in the atmosphere and in the sump and suspended in the sump water. Their transport takes place according to the prevailing gas and water mass flows (e.g. transport between zones from THY, deposition inside zones from AERIKA). So, all relevant processes relating to the fission products and the different carriers are considered: deposition of aerosol particles by natural processes or aided by technical systems such as filters and spray systems, washing-off from walls, and carrier change due to radioactive decay.

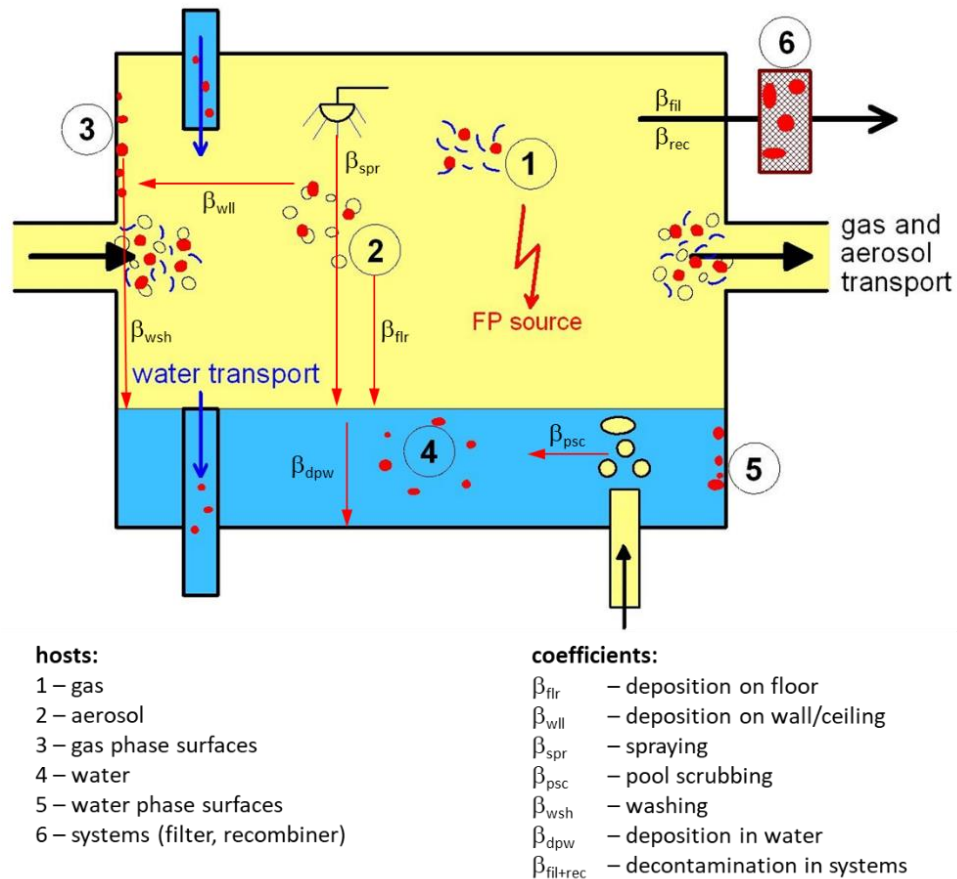


Fig. 1.5 FIPHOST zone, fission product hosts modelled in COCOSYS

Nuclide behaviour in COCOSYS is simulated with the **FIPISO** module /HES 98/. FIPISO considers the reactor's initial core inventory (pre-calculated by other codes) and calculates on this basis the decay of the fission products according to the time of the onset of the release by using established nuclide libraries (analogous to ORIGIN). Typically, between 400 and 600 different nuclides are considered in the calculation. The transport of nuclides is calculated by FIPHOST, too. The decay energy in the individual zones and on the individual carriers is considered in the THY main module.

The complex chemistry in the iodine module **AIM** /WEB 09/ contains approx. 70 different reactions. AIM distinguishes between 17 iodine species in the atmosphere and 11 iodine species in the sump. It calculates iodine transport between atmosphere and sump as well as across the compartments as depicted in Fig. 1.6. The impact of engineered systems (filter, spray, etc.) on the iodine behaviour is modelled. The behaviour of the particulate aerosol species CsI and AgI is

taken over from the AERIKA model. The AIM iodine module was tested and improved on various THAI experiments. This helped in particular to improve the interactions of I_2 on steel surfaces.

- A) Chem. iodine reactions and ad-/desorption processes**
- B) Interaction processes**
- (1) **Thermal hydraulic** boundary conditions and inter-compartmental gas and water transport
 - (2) **Iodine decay heat and dose rate** feedback on th/hy, aerosol behaviour and chem. reactions
 - (3) **Aerosol behaviour** of particulate iodine species

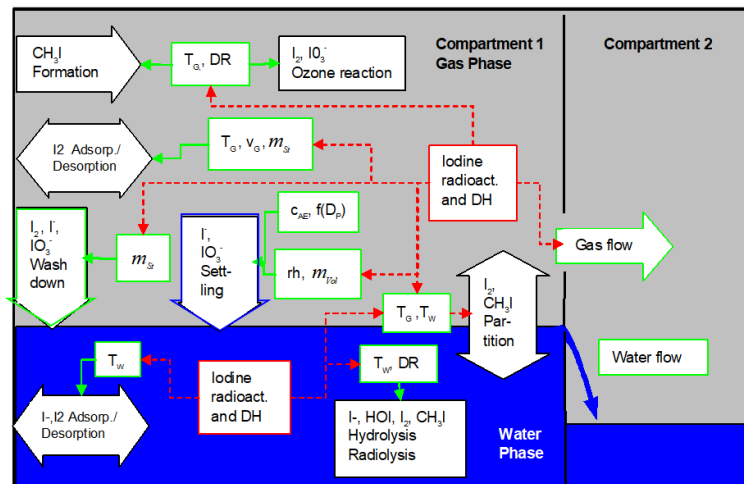


Fig. 1.6 AIM model in COCOSYS – iodine interaction with thermal hydraulics and aerosols

1.3 Behaviour of corium and concrete

In case of a reactor pressure vessel failure during a severe accident, the molten core would drop onto the concrete base structure of the containment. The interaction of the core melt with concrete could continue for a long period of time. During this, a number of phenomena are important for the subsequent course of the accident. The simulation of the following phenomena and processes is subject of the COCOSYS main module **CCI** for corium-concrete interaction:

- concrete decomposition,
- release of steam and gases from the decomposing concrete,
- chemical reactions of these gases and of the molten concrete constituents with metallic constituents of the melt and within the containment atmosphere,
- dilution of the molten fuel materials by molten concrete constituents and evolution of the freezing behaviour of the molten pool,
- aerosol and fission product release.

CCI is based on the code MEDICIS, which was originally developed by IRSN and GRS for the integral code ASTEC /CRA 05/. It uses a lumped parameter approach with layer-averaged heat and mass balances and considers either one homogeneous pool with well-mixed metal and oxide melt fractions, or - as shown in Fig. 1.7 - a stratified configuration of two layers with metal at the bottom and oxide on top (or vice versa). Using the configuration evolution option, the pool may evolve with time from an initial homogenous pool to a stratified configuration depending on a stratification criterion. In this criterion the superficial gas velocity through the pool is an important model parameter, derived from BALISE experiments. For each layer present, mass balance equations are solved per chemical element and the layer temperature is then computed from the energy balance equation considering the specific enthalpies of chemical species composing the layer's mass. The energy balance equation including metal oxidation reactions is solved using a consistent set of enthalpy functions for all involved reactants and products.

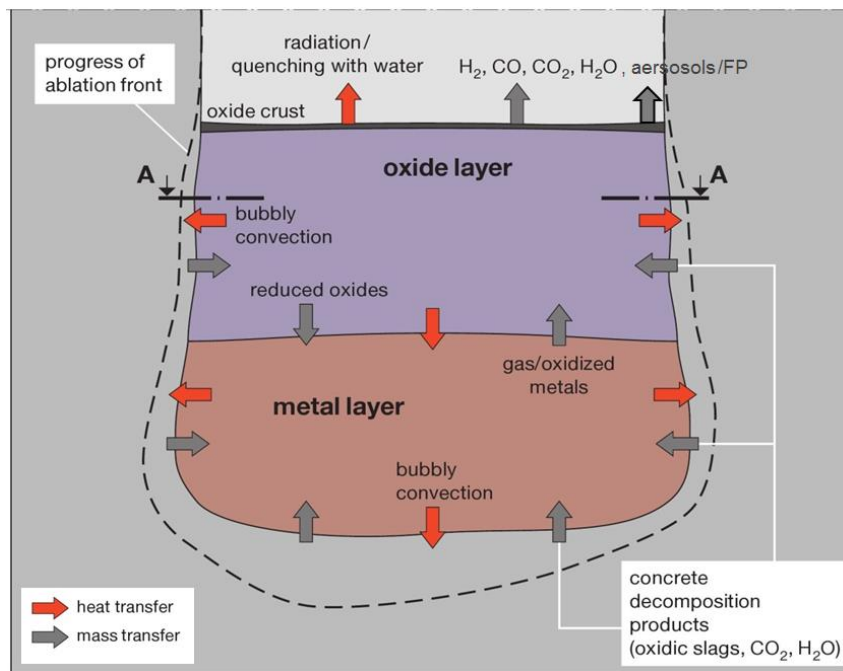


Fig. 1.7 CCI module in COCOSYS – stratified pool configuration

The 2D cavity geometry is assumed axisymmetric and is determined as function of time using the local energy conservation at each boundary node and a common melting approach (Stefan's equation) to evaluate the concrete ablation. Heat transfer between melt and concrete is calculated on the basis of a distribution of effective heat transfer coefficients along the pool interface in combination with a concrete decomposition temperature. These effective heat transfer coefficients (a proposed set of empirical heat transfer coefficients derived from experiments) are representative for the overall heat transfer from the bulk to the interfaces and are valid for the concrete decomposition temperature specified. The upward heat transfer from the upper interface of the pool (including a potential top crust) to the surrounding is calculated considering radiation and convection processes. A simplified model considers the formation of a quasi-steady upper crust under dry conditions. In case of top flooding conditions, the model equates the heat flux through a potential top crust with the heat flux obtained from the approximated boiling curve.

The thermo-physical properties of chemical elements and compounds forming the corium and the concrete basemat are taken from a material data base /BAR 07/.

Fission product release from the molten corium concrete pool is approximated assuming thermodynamical equilibrium between gas bubbles released from concrete decomposition and the melt /KÓŠ 07/.

Interactions with the main modules THY and AFP are taken into account: in CCI boundary conditions in the cavity (pressure, temperature, concrete base structure) are transferred from THY, the release of steam and gases from the corium-concrete mixture as well as radiative and convective heat from melt surface determined by CCI are considered in THY, and the release of aerosols and fission products from the core-concrete interaction in AFP.

2 Status of validation, plant applications

According to the long tradition of investigations in the field of containment research in Germany, COCOSYS is validated on a wide spectrum of tests performed at German or international test facilities. The tests carried out at the former facilities Battelle Model Containment (BMC) and Heiß-Dampf-Reaktor (HDR) as well as the ongoing tests in the THAI facility form the backbone of the COCOSYS validation. The validation status is summarized in Tab. 2.1.

Most of the older tests are calculated knowing the experimental results, whereas a large part of the recent calculations is performed without any knowledge about the experimental results. From GRS point of view the predictive capability of a code and its user can only be demonstrated with so-called 'blind calculations'. In such kind of calculations, the user has to select the options available in the code. In blind calculations this selection is based on the user's experience and the quality of the models inside the code.

Tab. 2.1 Experimental tests being used for COCOSYS validation since the earlier code development

Phenomenon	Facility	Experiment
Thermal hydraulics	BMC	Rx4, C13, D3, D6, D17, F2, VANAM M3
	HDR	T31.3, T31.5, E11.2, E11.4
	THAI	TH1, TH2, TH7, TH9, TH10, TH13 (ISP-47), TH14, TH15, TH17, TH23, TH27, TH29, HM1, HM2 WH20
	TOSQAN / MISTRA	ISP-47 step 1 tests, MICOCO
	PANDA	T9, T9bis, T17
Hydrogen combustion	BMC	Ix2, Ix9, Hx26, VANAM M4
	HDR	E12.3.2
	NUPEC	B2-6, B8-3
	ENACEFF	RUN765
	THAI	HD-2R, HD-15, HD-22, HD-24
Passive Autocatalytic Recombiner	BMC	Gx4
	HDR	E11.8.1
	THAI	HR-2, HR-35, HR-40, HR-41, HR-42
Spray systems	BMC	PACOS Px1
	HDR	E11.1
	MISTRA	MASP0, MASP1, MASP2
Passive systems / hydrodynamic	PANDA	BC3, BC4, PC1, ISP-42 tests, A, D, E and F
	BC-V213	LB LOCA test 1, SLB-G02
	GKSS	M1
	MARVIKEN	M19, M24

Phenomenon	Facility	Experiment
	THAI	WH-20
Jets and plumes	BMC	HYJET Jx2
	THAI	TH7, TH10, TH13, HM2
	PANDA	OECD-SETH T9, T9bis, T17
Pyrolysis ^{D)}	HDR	E41.7, E42.1 E42.2
	NIST	more than ten tests of ICFMP No. 3
	OSKAR	ICFMP No. 4: tests T1 and T3 ICFMP#5-T1, -T3
	DIVA	OECD PRISME: PRS-SI-D1, PRS-SI-D3, PRS-SI-D6 PRS-LK-D1, PRS-LK-D2, PRS-LK-D4 PRS-INT-D1, PRS-INT-D2, PRS-INT-D4, PRS-INT-D5, PRS-INT-D6 PRS2-VSP-D2, PRS2-FES-D1, -D2
Aerosol behaviour	BMC	VANAM M2*, M3 (ISP-37), M4
	KAEVER	~ 11 tests, ISP-44
	THAI	Aer-1, Aer-3, Aer-4, AW-1, AW-2, AW-3 (part 1), AW-3 (LAB), AW-4, TH-14 – TH-17
Iodine chemistry	RTF	3B, P9T1, P10T1, P10T3, RTF1, RTF3, RTF5 OECD BIP: G-1, G-13 OECD BIP: G-4, ... G-12 OECD BIP: A-7, A-9
	EPICUR	S1-3, S1-4, S1-5, S1-11, AER1, AER2
	THAI	AW-3 (part 2)
	RTF	ACE3B, PHEBUS RTF 3, PHEBUS-5, P9T1, P10T1, P10T3
	RTF-ISP41	PT02, P1T1, PHEBUS-1
Iodine transport behaviour	CAIMAN	ISP-41 tests: 97/02, 01/01, 01/03
	THAI	Iod-6 ... Iod-30
Integral fission product tests	PHEBUS	FPT1, FPT2, FPT3
Pool scrubbing		EPRI-II series POSEIDON PA test series
Venting filter	ACE	Aerosols: AA-19, AA-20
Molten corium-concrete interaction (mostly performed in stand-alone mode)	BETA	V1.8, V3.3, V5.1, V5.2
	ANL	ACE: L1, L6, L8 MACE: M3B, M4 OECD-MCCI: CCI-2, CCI-3, CCI-4, CCI-5
	COMET	L1, L2, L3
	MOCKA	3.1, 5.7, 6.3, 7.1

Phenomenon	Facility	Experiment
	VULCANO	VB-U5, VB-U6, VBES-U5
Melt spreading	KATS / ECOKATS	KATS tests No. 7, 14, 15, 17 and ECOKATS V1 and 1
	COMAS	Tests No. 5a, EU2b, EU3a, EU4
	VULCANO	VE-U7
	FARO	L32S
Direct Containment Heating (DCH)	DISCO	D06 FH01 ... FH03 H1 ... H6 KH1 ... KH7 L04 ... L05

2.1 Examples of validation

Results of the following experiments used in the validation process of the COCOSYS code system are summarised:

For the main module THY:

- THAI TH-13 at the THAI test facility in Eschborn, Germany;
- EREC SLB-G02 at the BC V-213 test facility in Electrogorsk, Russian Federation.

For the main module AFP:

- BMC VANAM-M3 at the former BMC test facility in Frankfurt, Germany;
- THAI IOD-11 at the THAI test facility in Eschborn, Germany.

For the main module CCI:

- MOCKA 5.7 at the MOCKA test facility in Karlsruhe, Germany.

2.1.1 THAI TH-13

The experiment THAI TH-13 was part (step 2) of the international standard problem ISP-47 which was devoted to the assessment of lumped-parameter and CFD models in the area of containment thermal hydraulics. The test was focused on the formation and dissolution of light gas clouds in the dome of the test vessel injecting steam and helium (representing hydrogen) at different positions.

2.1.1.1 THAI test facility

The test THAI test vessel of 9.2 m height, a diameter of 3.2 m and a total volume of 59.3 m³ is shown in Fig. 2.1. Its outer wall is 22 mm thick. This way it provides a sufficient level of radiation protection and makes the vessel suitable for experiments with up to 14 bar and 180 °C. Thus, at THAI most thermal hydraulic conditions that are to be expected in reactor containments can be simulated. In the interior of the vessel there is an inner cylinder which is open at the top and the bottom. Around the inner cylinder four condensate trays are positioned which reduce the effective opening in the annulus by two thirds. On the outside of the vessel three cooling / heating jackets are placed.

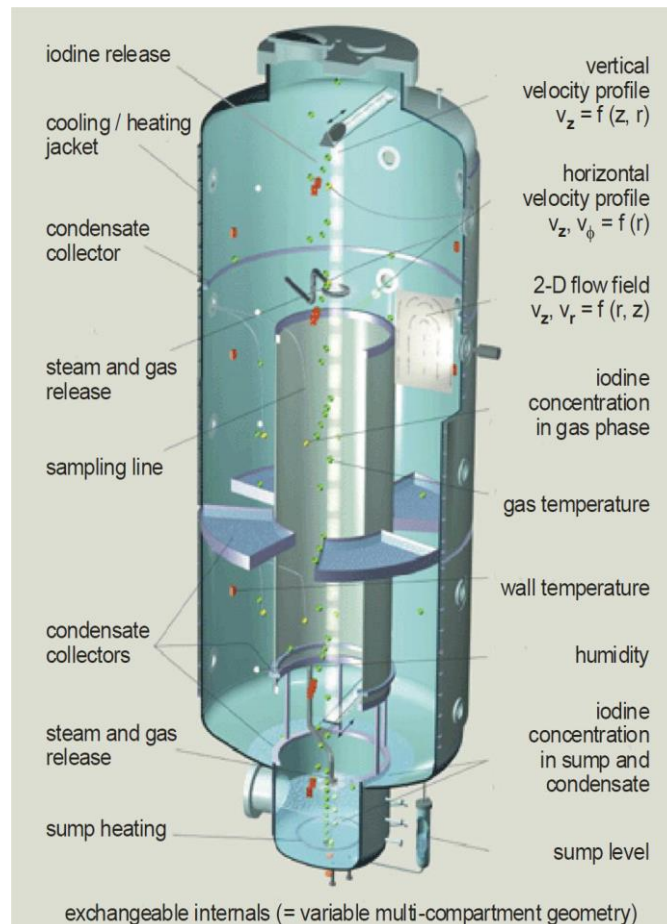


Fig. 2.1 THAI vessel and typical instrumentation /BEC 20/

Condensate can be collected in gutters (one positioned in the upper part of the vessel at the outer wall, two more a located at the lower part of the inner cylinder); it can be drained from the vessel for further analyses. This also applies for the collected condensate in the trays. Condensate can also be kept away from the main sump by a wall up to 100 mm high at the brink to the sump.

2.1.1.2 Experimental procedure of TH-13

Starting conditions were:

- pressure: 1.011 bar
- atmosphere temperature inside vessel: 20.6 ± 0.5 °C
- relative humidity inside vessel: 70.6 ± 3.4 %
- wall temperature: 20.6 ± 0.5 °C
- surrounding temperature: 22.7 ± 1.3 °C

The experiment comprised the following 4 phases:

- I. 0 – 2700 s**
Vertical helium jet injection in the upper part of the vessel ($z = 5.8$ m, 0.59 g/s).
- II. 2700 – 4700 s**
Vertical steam jet injection at the upper injection nozzle ($z = 5$ m, 35 g/s).
- III. 4700 – 5700 s**
Horizontal steam plume injection at the lower injection nozzle ($z = 1.28$ m, 35 g/s).
- IV. 5700 – 7700 s**
No injection.

2.1.1.3 COCOSYS model

The COCOSYS nodalisation for the THAI TH-13 experiment consists of 52 zones arranged in 15 layers (Fig. 2.2).

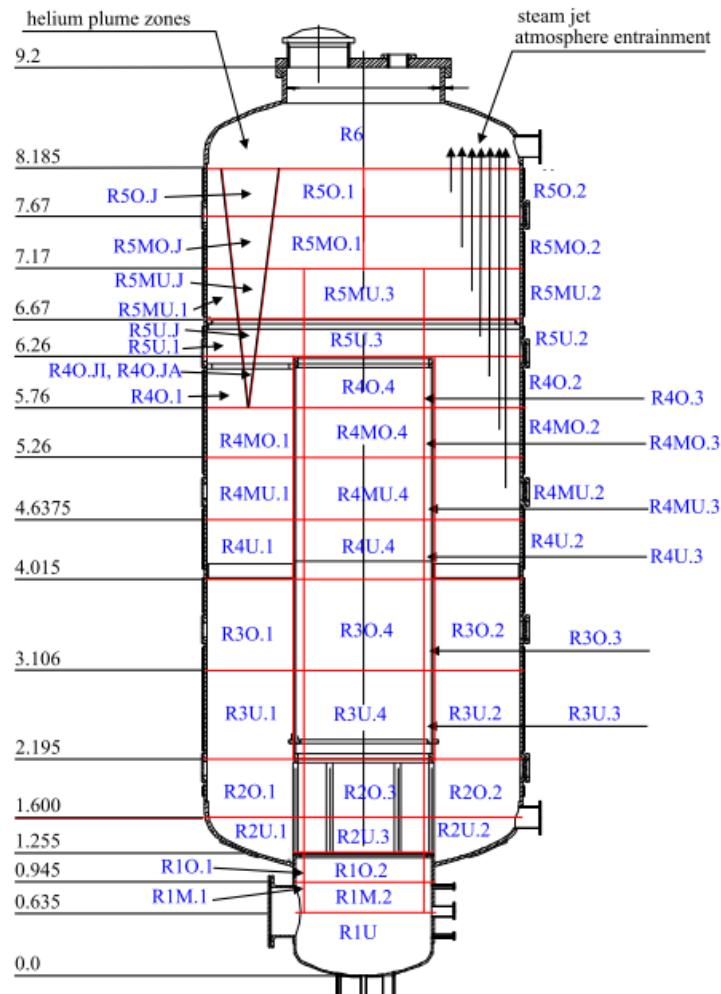


Fig. 2.2 THAI TH-13, COCOSYS nodalisation scheme

2.1.1.4 Selected results of validation

Exemplarily for the TH-13 test, results for pressure and helium concentration are presented.

The pressure in the vessel dome increases initially due to the helium injection (Fig. 2.3). At 2700 s, after starting the upper steam injection and at 4700 s, with begin of the lower steam injection, the pressure rises faster, because the steam partial pressure increases until a quasi-steady equilibrium between steam injection and condensation at walls is reached. Later on, pressure increases with a lower rate due to air partial pressure rise caused by the increasing temperature. In phase IV starting at 5700 s the pressure drops due to steam condensation.

In phase I, the He concentration in the upper plenum at 7.7 m (Fig. 2.4) increases due to the injection. It remains high for the rest of the experiment. Almost no He reaches the lower plenum until the start of the lower steam injection in phase III at 4700 s. Then the vessel atmosphere is mixed gradually as shown by the increase of the He content in the lower plenum at 1.6 m.

Generally, the COCOSYS results are in good agreement with the experimental data.

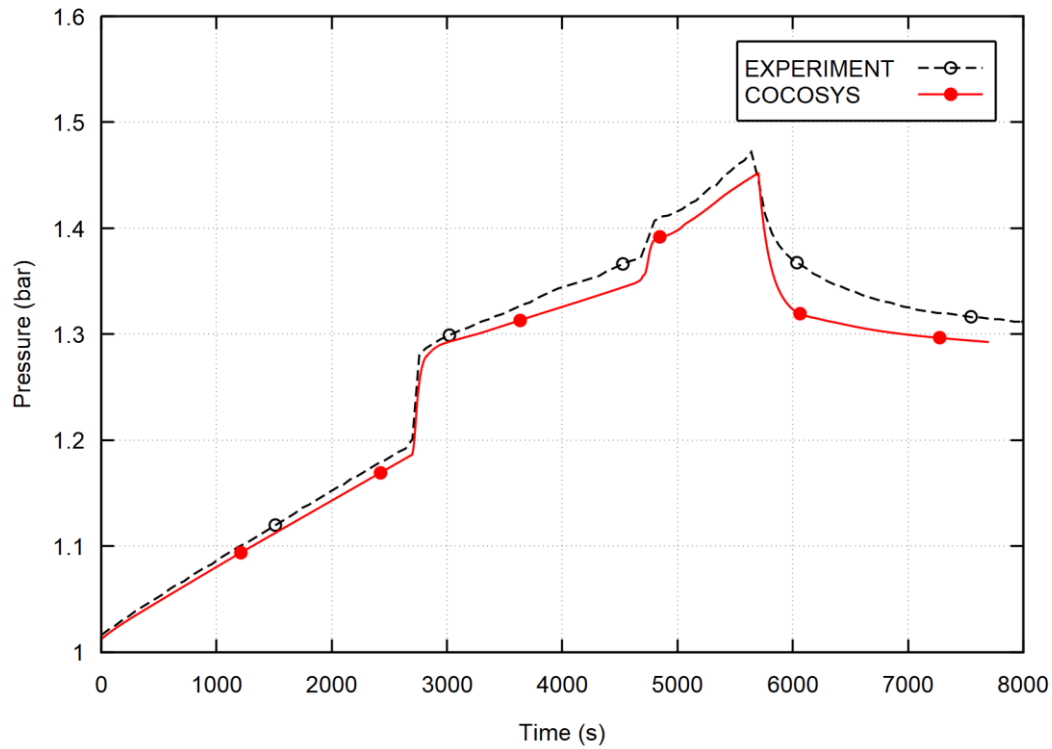


Fig. 2.3 THAI TH-13, pressure in upper dome zone

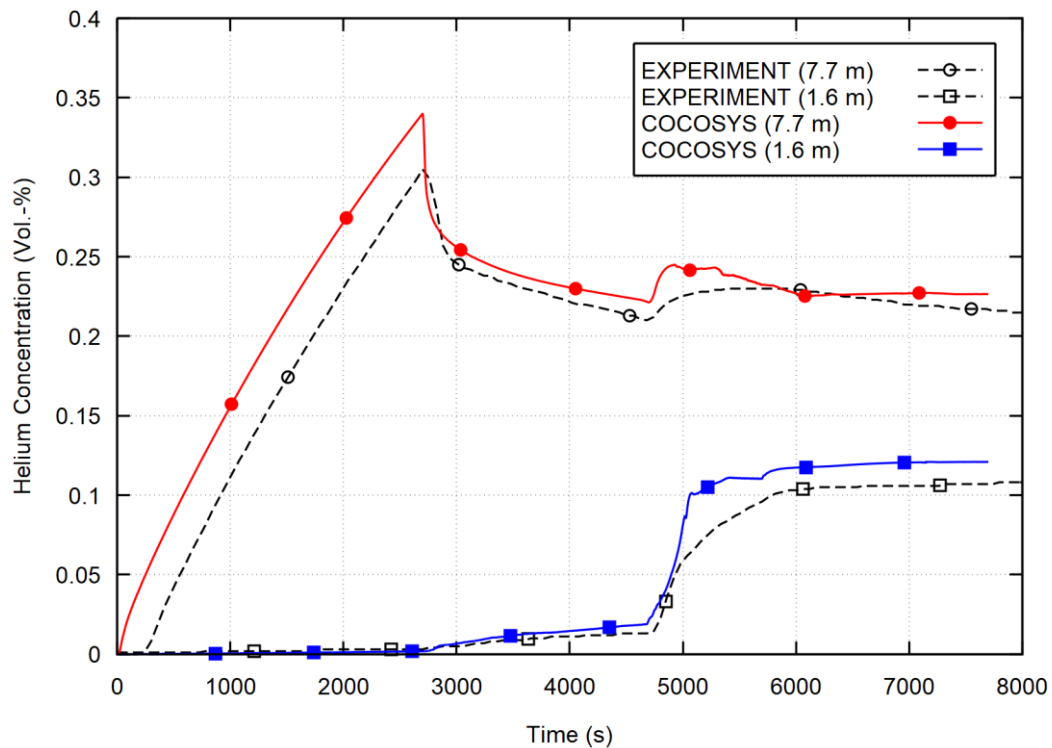


Fig. 2.4 THAI TH-13, helium concentration in upper and lower zones

2.1.2 EREC SLB-G02

The SLB-G02 test was designed to investigate the behaviour of the Bubble Condenser (BC) of NPPs with VVER-440/213 in case of a steam line break. The aim of the COCOSYS calculations was to validate the code for these specific conditions. In October 2002, the SLB-G02 test was performed at the BC V-213 facility of the Russian research centre EREC in Elektrogorsk /MEL 03/.

2.1.2.1 EREC BC V-213 test facility

The large-scale BC V-213 test facility (Fig. 2.5) consists of a high-pressure vessel system, hermetic compartments (e. g. steam generator box), an original module of the BC and the so-called air trap. The test facility was scaled 1:100 relative to the containment volume of a VVER-440/213. Its total volume amounts to about 520 m³ including 13 tons of water in the BC module. The BC module comprises two segments with nine full-scale gap-cap units each. The test facility is equipped with about 250 gauges to measure temperatures, pressures, differential pressures, mass flow rates, levels, humidity and relief valve opening angle.

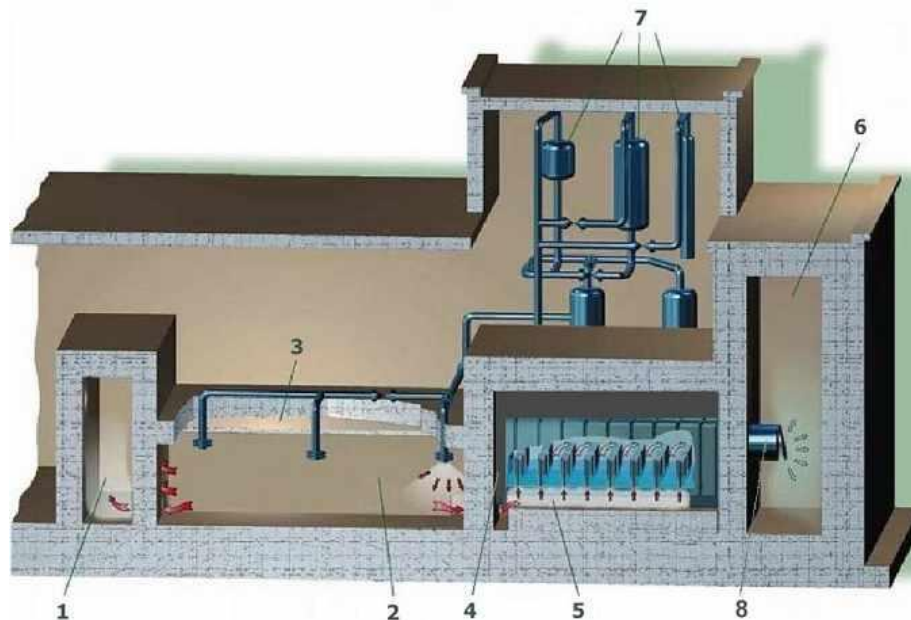


Fig. 2.5 BC V-213, schematic view of the test facility

- | | |
|--|---------------------------------|
| 1 – dead end volume (V0 in Fig. 2.6) | 5 – bubble condenser (V4) |
| 2 – steam generator box with three possible break locations (V1) | 6 – air trap (V5) |
| 3 – steam generator box (V2) | 7 – high-pressure vessel system |
| 4 – bubble condenser shaft (V3) | 8 – check valve |

2.1.2.2 Experimental procedure of EREC SLB-G02

The following features and parameters were determined by EREC to provide pressurise and temperature build-up in the hermetic compartment system characteristic for a steam line break in NPPs with VVER-440/213:

- coolant release through 4 vessels (Vv1, Vv2, Vv3 and Vv5) of the high-pressure vessel system;

- initial water level in Vv1: 2.225 m, in Vv2: 1.270 m;
- nozzle diameter: 56 mm;
- pressure in vessels Vv1, Vv2, Vv3 and Vv5: 4.7 MPa;
- temperature in vessels Vv1, Vv2, Vv3 and Vv5: 260 °C (T_{sat});
- additional supply of slightly superheated steam (30 bar, 270 °C) into vessel Vv1 with a mass flow rate 0.4 kg/s from 100 s to 500 s and 0.2 kg/s after that.

The duration of the test was 30 minutes. The specified break location was the nozzle afar from the BC segments. To reduce uncertainties in the initial conditions the test was started with "cold" conditions of about 20 °C, i.e. without test facility pre-heating.

2.1.2.3 COCOSYS model

The dataset for the post-test calculations with COCOSYS comprises 24 nodes, 35 atmospheric junctions, 21 drainage junctions and 109 heat conduction structures. The nodalisation scheme is presented in Fig. 2.6. The mass and energy release rate was calculated with the GRS code ATHLET using the values measured for the high-pressure vessel system.

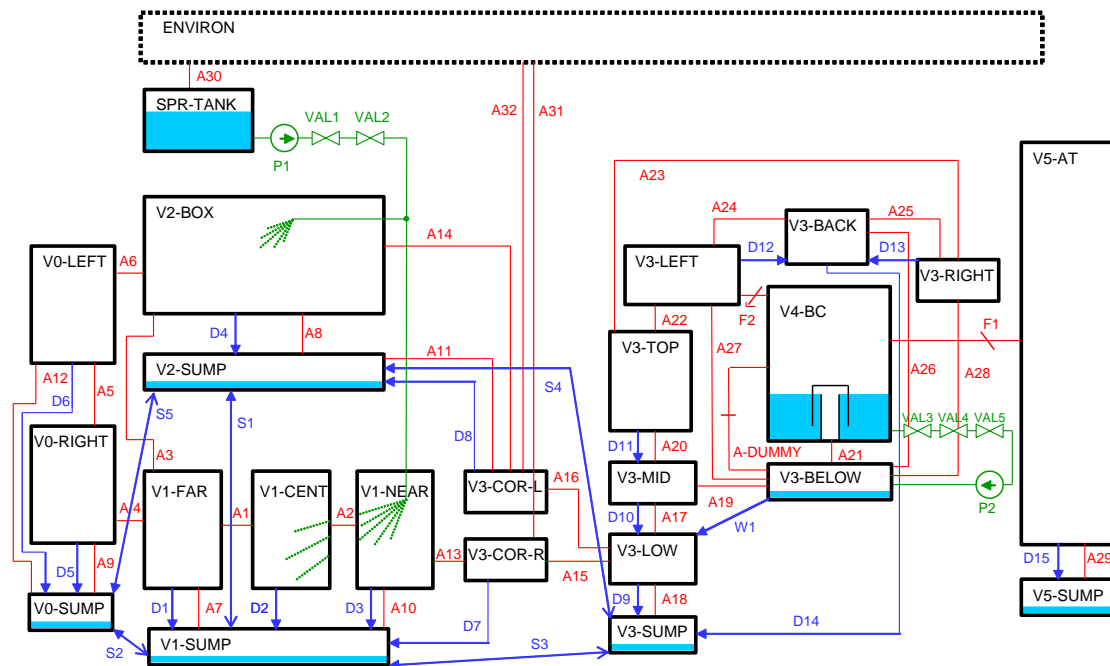


Fig. 2.6 EREC SLB-G02, COCOSYS nodalisation with 24 zones

2.1.2.4 Selected results of validation

Exemplarily for the SLB-G02 test, the comparison of measured and calculated pressure in three selected zones and of the water temperature in the right side of the BC pool is presented.

In Fig. 2.7 the calculated pressures for compartments V1, V4 and V5 are compared with the experiment. The pressure behaviour is good post-calculated, i.e. the calculation is mostly in-side the uncertainty bandwidth, which is given as ± 4 kPa.

In the short-term up to 50 s the calculated pressure increase is somewhat too high. This effect was calculated in the frame of different projects for other EREC BC V-213 tests too, also by all other used codes as e.g. CONTAIN and WSPLESK. In the period of 150 – 400 s the calculation results for V1 and V4 are at the upper uncertainty band. The calculated pressure in the air trap leaves the uncertainty range after 600 s, the pressure decrease is lower than the measured one.

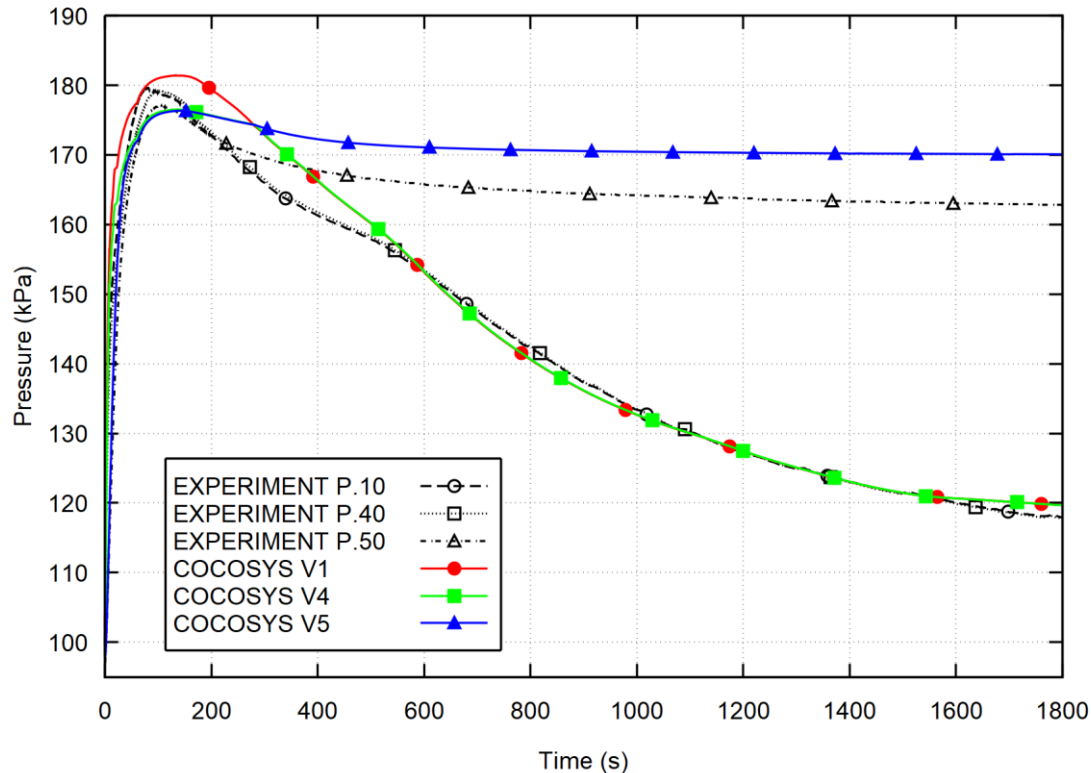


Fig. 2.7 EREC SLB-G02, pressure in compartments

The calculated and measured heat-up of the water is given exemplarily for the right side of the BC pool in Fig. 2.8. Due to the simulation of the BC fragment by one COCOSYS node an average pool water temperature is calculated.

The performed validation activities for VVER-440 BC show that COCOSYS is capable to post-calculate the SLB-G02 test. The main parameters were well calculated by COCOSYS, e.g. the maximum pressure and the water in the Bubble Condenser trays. As result of this analysis the material properties of the reinforced concrete, the opening behaviour of the relief valve between BC and BC shaft, and the modelling of the wooden insulation (special feature of the test facility) were identified as parameters of main influence.

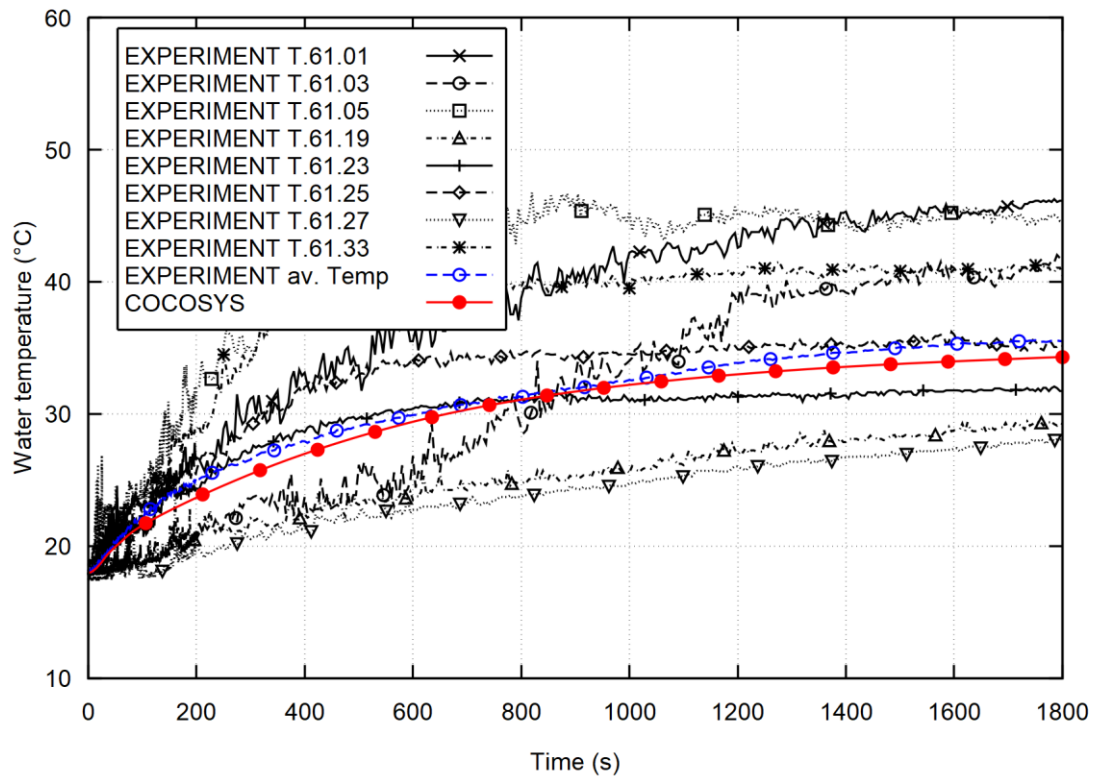


Fig. 2.8 EREC SLB-G02, water temperature in zone V4-BC

2.1.3 BMC VANAM-M3

The VANAM tests were performed at the Batelle Modelle Containment in Frankfurt. First of all these tests were aimed at code validation. In the test VANAM-M3 the hygroscopic aerosol material NaOH was utilized in order to investigate effects of atmosphere stratification and mixing. This test was investigated in the international research activities as standard problem ISP-37.

2.1.3.1 BMC Test facility

The Battelle Model Containment has a free volume of 626 m³. It was built rotationally symmetric of reinforced concrete and is subdivided into several compartments. The VANAM test geometry (Fig. 2.9) resembles a PWR containment.

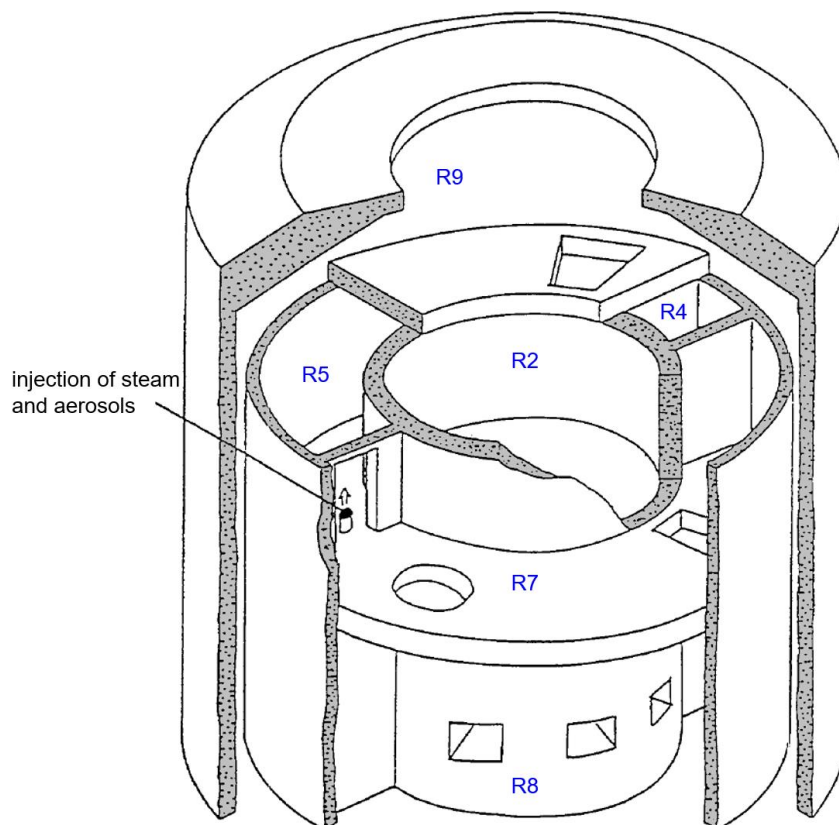


Fig. 2.9 BMC VANAM, schematic view of the test facility

2.1.3.2 Experimental procedure of VANAM-M3

The experimental procedure of the VANAM-M3 test is oriented on the core melt scenario ND* according to the German Risk Study phase B. The test was subdivided into the following 6 phases:

- I. 1.13 to 17.2 h**
The test facility is heated up and the initial boundary conditions are adjusted: Steam is injected into R5 to get a constant containment pressure of 1.25 bar. At the beginning of phase I there is a controlled air removal out of R9 (annulus) lower part, leading to steam entry into this region and heating up the structures. Towards the end of phase I, air is re-injected into the lower annulus region in order to get the desired air content.
- II. 17.2 to 18.23 h**
2.21 kg of the soluble, hygroscopic aerosol NaOH suspended in a steam-air mixture is injected into R5. The containment pressure rises to 2.05 bar.
- III. 18.23 to 22.7 h**
No injection. Pressure decreases to 1.25 bar, because of the steam condensation on the outer containment wall.
- IV. 22.7 to 23.14 h**
Second injection of NaOH aerosol (0.719 kg) suspended in a steam-air into R5. The pressure increases.
- V. 23.14 to 25.26 h**
For the first 10 min all injections are stopped. Then steam is injected into the lower central room R3. The pressure increases to about 1.7 bar.
- VI. from 25.26 h**
The steam injection is switched back to R5. The pressure stabilizes at about 1.7 bar.

2.1.3.3 COCOSYS model

The COCOSYS model for the VANAM-M3 calculations consists of 15 zones (inclusively one environmental zone), 28 junctions and 53 structures. The nodalisation scheme is shown in Fig. 2.10:

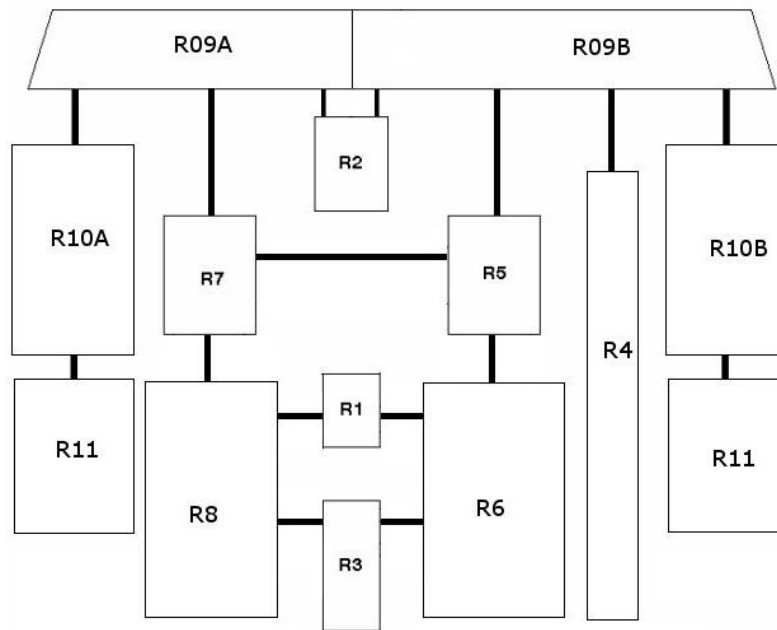


Fig. 2.10 BMC VANAM, COCOSYS nodalisation scheme

2.1.3.4 Selected results of validation

Exemplarily for the VANAM-M3 test, the comparison of measured and calculated pressure and aerosol concentration in the upper part of the BMC annulus (compartment R9) is presented.

Fig. 2.11 shows the pressure comparison for the annulus upper part. Between 5 and 15 hours and after 24 hours, the calculated pressure is overestimated due to the non-consideration of the BMC leakages. The pressurisation, the depressurisation and the maximum pressure in phases I to V fit good with the measured results.

Fig. 2.12 presents the calculated aerosol concentration in the upper part of the BMC facility against the M3 experimental data. The COCOSYS result agrees well with the measured concentration.

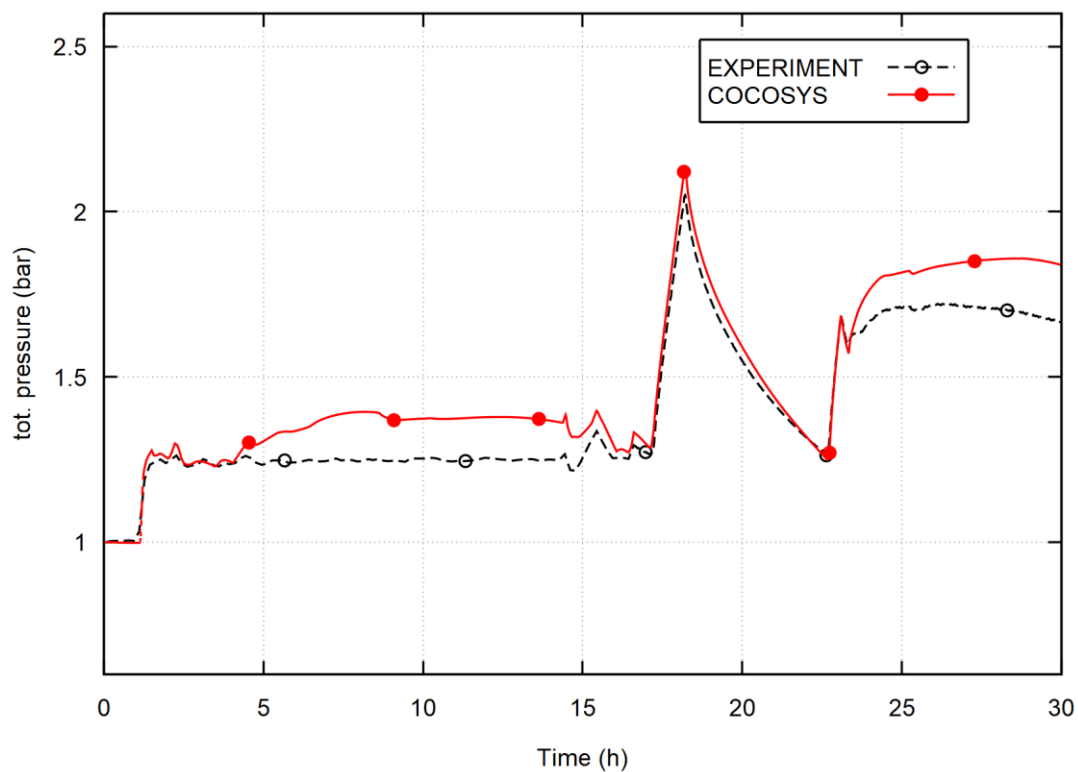


Fig. 2.11 BMC VANAM-M3, pressure in the upper annulus region

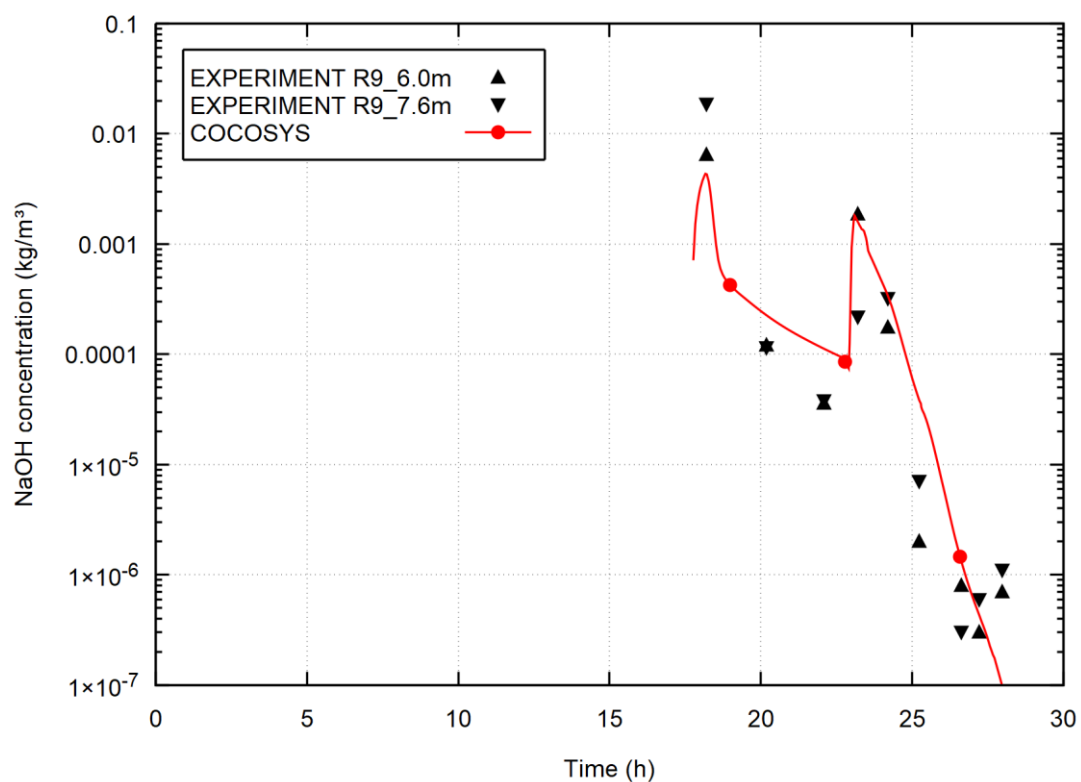


Fig. 2.12 BMC VANAM-M3, aerosol concentration in the upper annulus region R9

2.1.4 THAI lod-11

In 2004, the multi-compartment test lod-11 was performed at the THAI facility to investigate the transport behaviour of molecular iodine (I_2). In this test a non-homogeneous iodine concentration in the atmosphere was simulated. A benchmark analysis on THAI test lod-11 was part of the European project SARNET2.

2.1.4.1 THAI test facility

A general outline on the THAI test facility is given in section 2.1.1.1.

With respect to validation activities of the COCOSYS main module AFP, it is to be added, that the test rig is equipped with supply systems for steam, compressed air, nitrogen, oxygen, helium, hydrogen, aerosols and gaseous iodine.

For the test lod-11, the THAI vessel was subdivided into five compartments: bottom compartment with main sump, lower annulus, upper annulus, central compartment and dome compartment (Fig. 2.13).

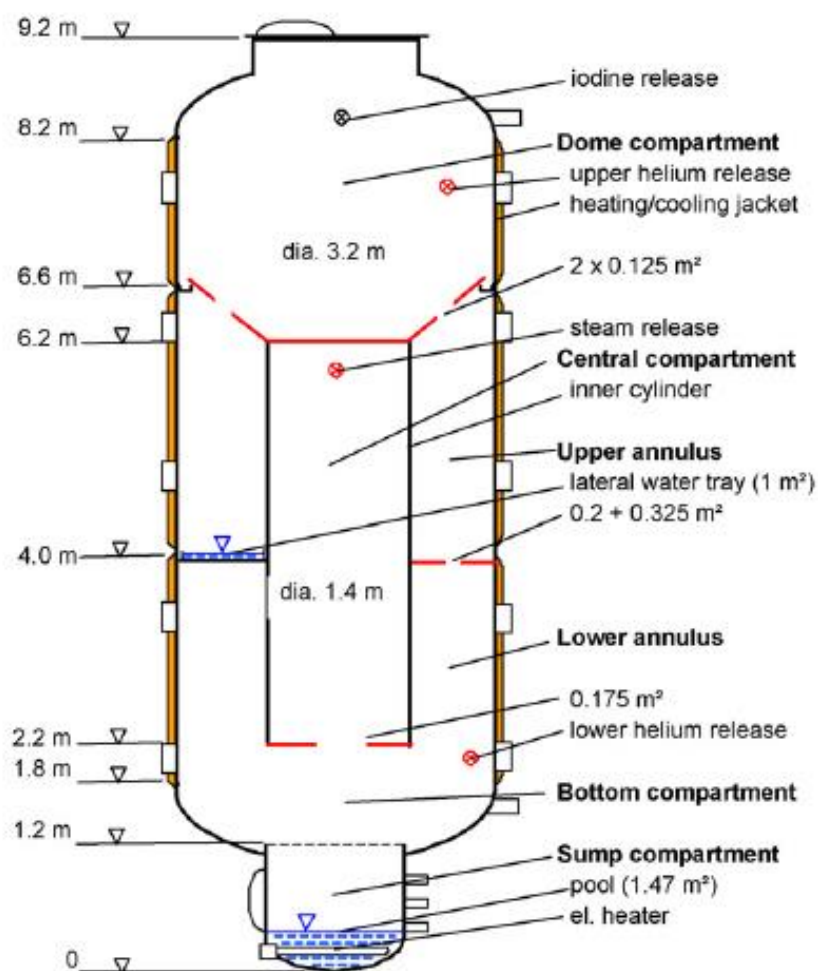


Fig. 2.13 THAI vessel, 5-compartment geometry for lod-11 test

2.1.4.2 Experimental procedure of THAI Iod-11

In Iod-11 molecular iodine (I_2) was injected into the dome compartment, steam into central and helium into bottom compartment. The test procedure comprised the following 4 phases:

I. Preparation phase

A special wall heating and cooling procedure established a stable gas and temperature stratification. At the end of this phase the atmosphere temperature in the dome compartment was about 90 °C and that in the lower compartments between 50 °C and 18 °C, which was the sump water temperature. The pressure was somewhat higher than the ambient pressure.

II. Stratification phase (0 to 5.32 h)

A stable atmospheric stratification was maintained. At the beginning about 1 g I_2 was released into the dome by a puff of carrier gas. The beginning of the release marks the start of the experimental time ($t = 0$). A significant portion of the released I_2 was adsorbed at the steel surfaces in the dome.

III. Transition phase (from 5.32 h on)

Transition to a mixed vessel atmosphere. The two lower jackets were heated, and helium was injected into the bottom compartment. The gas temperatures varied between 70 °C and 80 °C. I_2 was transported from the dome to the upper annulus and from there further down.

IV. Well-mixed phase

Long-term phase with quasi steady-state conditions. Only little heat was injected to maintain natural convection and mix the atmosphere. I_2 was continuously desorbed from the dome structures and transported into the lower compartments. The atmospheric temperature differences were relatively small.

2.1.4.3 COCOSYS and AIM models

For the investigation of the iodine behaviour with COCOSYS inclusively the AIM model of the main module AFP, two nodalisations are needed. The left part of Fig. 2.14 depicts the nodalisation of the THAI vessel used for the COCOSYS calculations. The iodine compartments for the AIM model are given on the right side of this figure.

The COCOSYS nodalisation comprises 46 zones interconnected by 73 atmospheric junctions. The dome compartment (DC) is subdivided into seven zones to simulate stratification processes there. The lower and the upper annulus (LA, UA) are subdivided axially to calculate counter current flows. Two zones model the external tanks (LCT, UCT), which collect the wall condensate, and two other zones represent the environment. 58 heat-conducting structures model the vessel walls and internal structures.

For the iodine calculation the thermal hydraulic nodalisation was condensed to 13 iodine compartments by combining several zones into one iodine compartment. This COCOSYS-AIM feature takes into account the different spatial accuracy requirements of the modules and reduces the calculation time.

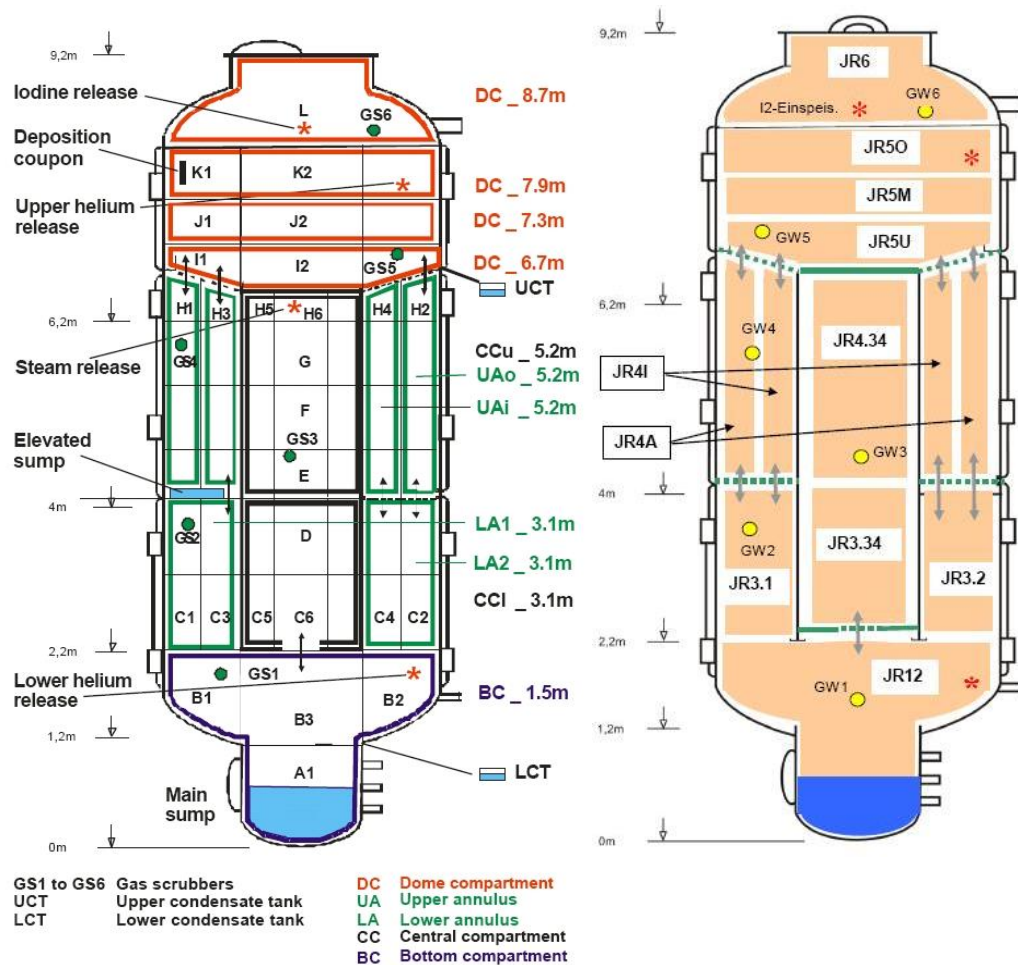


Fig. 2.14 THAI Iod-11, COCOSYS nodalisation (left) and AIM nodalisation (right)

2.1.4.4 Selected results of validation

Exemplarily for the Iod-11 test, results for concentrations of helium and gaseous iodine are presented.

Fig. 2.15 shows the helium concentration at elevations 1.7 m and 8.7 m. The injection starts after 5.32 h in the lower part of the THAI facility. Thus, the helium concentration reaches a maximum value of about 13 % at elevation 1.7 m after 6 h. At elevation 8.7 m, the concentration rises over a period of about 3 h. At about 8 h, an almost homogenous mixing of helium is reached with an overall concentration of 10 %.

The behaviour of gaseous iodine I_2 is illustrated in Fig. 2.16. It shows that the iodine remains stratified until the beginning of the transition phase. The measured iodine concentration is about 10^{-5} g/l at elevation 8.3 m, while it goes up to only $3 \cdot 10^{-8}$ g/l at elevation 1.8 m. The iodine stratification remains stable for a longer time in comparison to the mixing of the helium concentrations. After 7 h, the concentration is $3 \cdot 10^{-6}$ g/l at elevation 8.3 m and only $3 \cdot 10^{-7}$ g/l at elevation 1.8 m. After 10 h it is $8 \cdot 10^{-7}$ g/l at 8.3 m and 10^{-7} g/l at 1.8 m. Afterwards, no measurements have been taken until 23 h. At this time, the mixing of the iodine is proceeded and the difference of the iodine concentration between both positions is reduced to a factor of 2 and the iodine concentration has decreased to about 10^{-7} g/l in the whole facility.

Generally, with respect to the concentrations of helium and gaseous iodine, the results of the COCOSYS calculation are in good agreement with the experimental results.

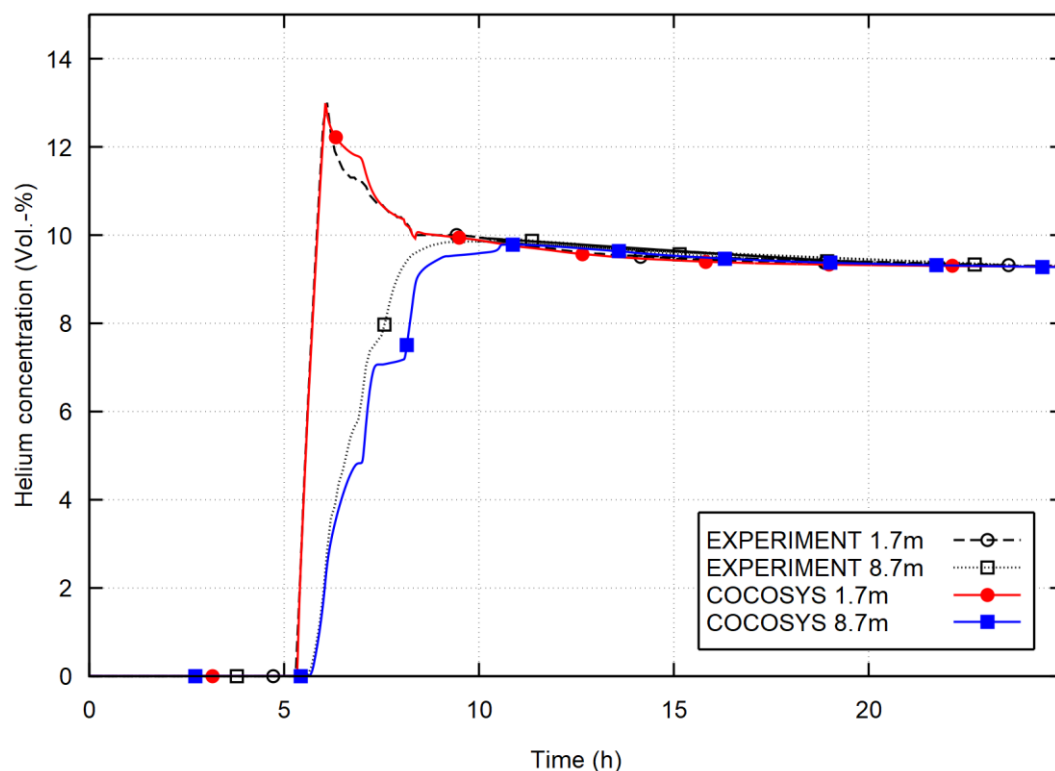


Fig. 2.15 THAI Iod-11, He concentration in a lower (1.7 m) and an upper zone (8.7 m)

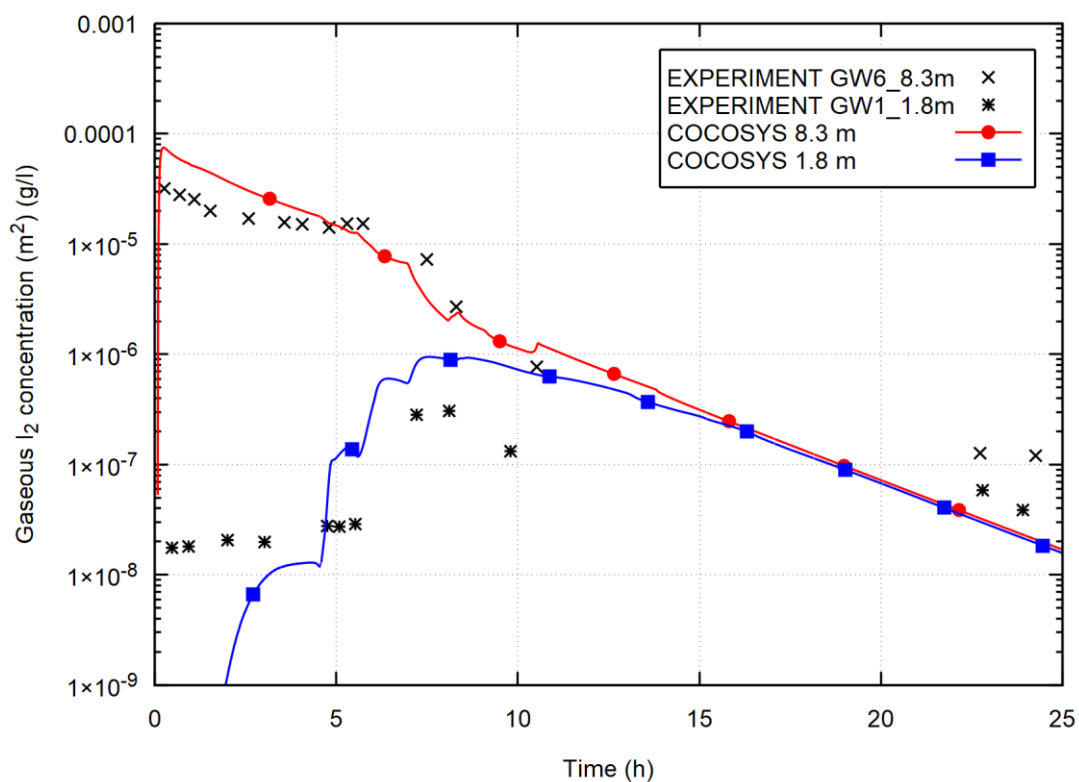


Fig. 2.16 THAI Iod-11, gaseous iodine concentration at different levels

2.1.5 MOCKA 5.7

MOCKA experiments serve to study the interaction of core melt simulant oxide (Al_2O_3 , ZrO_2 , CaO) and metal melt (Fe) in a stratified configuration with different types of concrete typical for reactor cavities. Unlike other molten core-concrete interaction (MCCI) tests, molten corium and concrete are heated-up by means of chemical reactions with thermite ($\text{Fe}_3\text{O}_4 + \text{Al}$) and zircaloy. In test MOCKA 5.7 the influence of a 12 wt.-% reinforced concrete on the MCCI was investigated with focus on the corium-concrete configuration and its erosion behaviour.

2.1.5.1 MOCKA test facility

The MOCKA (Metal Oxide Concrete Interaction in Karlsruhe) test facility is an outdoor installation. Its main part - the test crucible - is located below the ground surface. Fig. 2.17 shows the entry to the test crucible and the construction for adding thermite/zircaloy to the crucible at the moment of its supply.

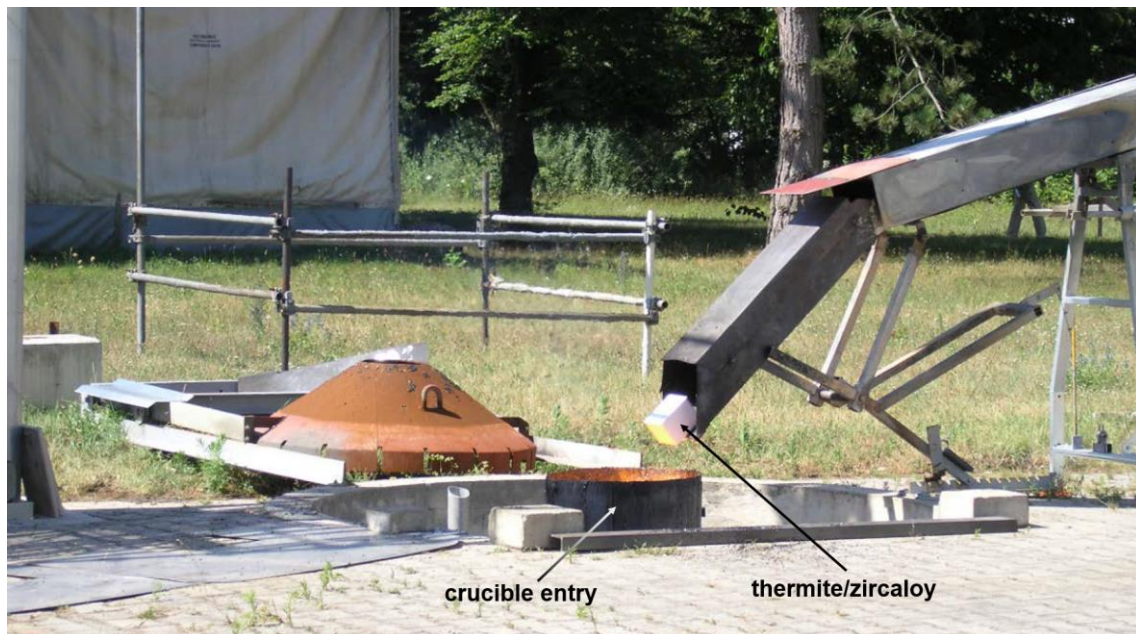


Fig. 2.17 MOCKA test facility /ISA 19/

2.1.5.2 Experimental procedure of MOCKA 5.7

The MOCKA 5.7 test was conducted in October 2015. A test specific crucible with instrumentation was installed. The experiment MOCKA 5.7 was conducted with a reinforced siliceous concrete crucible of 25 cm in diameter with an initial mass fraction of SiO_2 of about 62 % and a CaO fraction of ~12 %. The concrete cylindrical wall up to 70 cm from the bottom was made of siliceous concrete, whereas the cylindrical wall above 70 cm is made of inert material (ceramics).

The ignition of the thermite defines time $t = 0$ s for the MOCKA 5.7 test. The initial mass of thermite, including CaO amounted to 110.7 kg. After 3:10 min, the thermite reaction was completed. The additions of thermite and zircaloy started at 3:16 min and ended at 36:55 min.

In total 260 kg thermite and 95,4 kg zircaloy have been added during the experiment.

2.1.5.3 COCOSYS/CCI model

The activities of the MOCKA 5.7 post-test calculations were focused on the application of the CCI module in COCOSYS. Consequently, a simple 2 zone COCOSYS nodalisation including the CCI model as shown in Fig. 2.18 was applied.

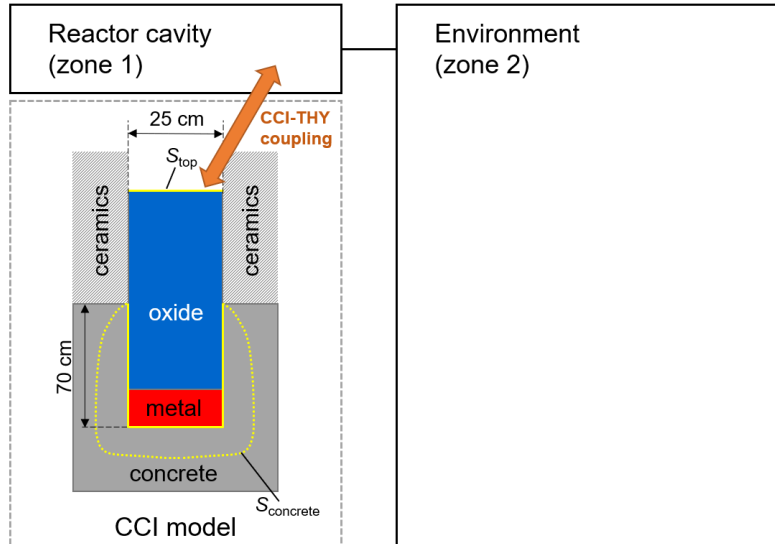


Fig. 2.18 MOCKA 5.7, COCOSYS nodalisation with CCI model

2.1.5.4 Selected results of validation

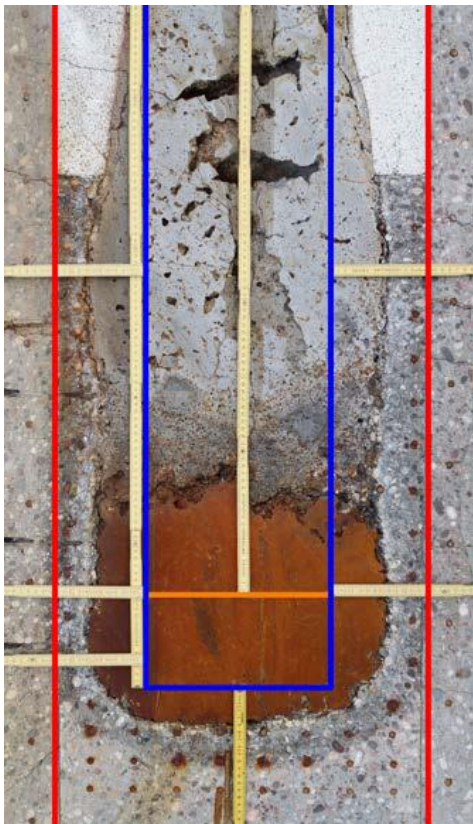


Fig. 2.19 MOCKA 5.7, vertical cut of test crucible after test /FOI 19/

Exemplarily for the MOCKA 5.7 test, the comparison of measured and calculated concrete erosion depths and oxide/metal phase temperatures is presented.

Due to the specifics of phenomena during interactions between molten core and concrete, and in context with the uncertainties accompanying corresponding tests, two kinds of experimental results were used in the COCOSYS/CCI validation process:

- a vertical cut of the test crucible showing the situation after concrete ablation due to the MCCI simulated in the MOCKA 5.7 test. The cut is shown in Fig. 2.19 with indication of the initial size of the crucible cavity (blue line). The orange line indicates the initial height (13 cm) of the metal melt and the red line marks the outer surface of the reinforced siliceous cylindrical crucible.
- results of the temperature measurements installed in the test crucible.

A comparison of the final ablated depths and the erosion volume determined from the cut of the test crucible and calculated by the CCI module of COCOSYS 3.0.1 is presented in Tab. 2.2.

Tab. 2.2 Comparison of MOCKA 5.7 data with COCOSYS/CCI results after 2000 s

Parameter	Experiment	CCI module (COCOSYS 3.0.1)
Total erosion volume, (l)	~ 54.0	64.3
Radial ablation by oxide layer, (cm)	~ 8.2	10.
Axial ablation by metal layer, (cm)	~ 4.0	7.25

So, the MOCKA 5.7 results showed a non-uniform ablation at the melt/concrete interface with a radial ablation by the oxide layer about 2 times higher than the axial ablation by the metal layer. With respect to the CCI results, it should be mentioned that they are outcome of a best-estimate calculation taking into account an estimation of the heat which was transferred from the crucible to the atmosphere.

Information from the temperature measurements were used twice. On the one site, the disappearance of their signal is an indicator for the contact of the particular gauge with the melt i.e. about the evaluation of the ablation depth. The results were compared with the averaged erosion depths calculated by COCOSYS/CCI and are shown in Fig. 2.20 and Fig. 2.21.

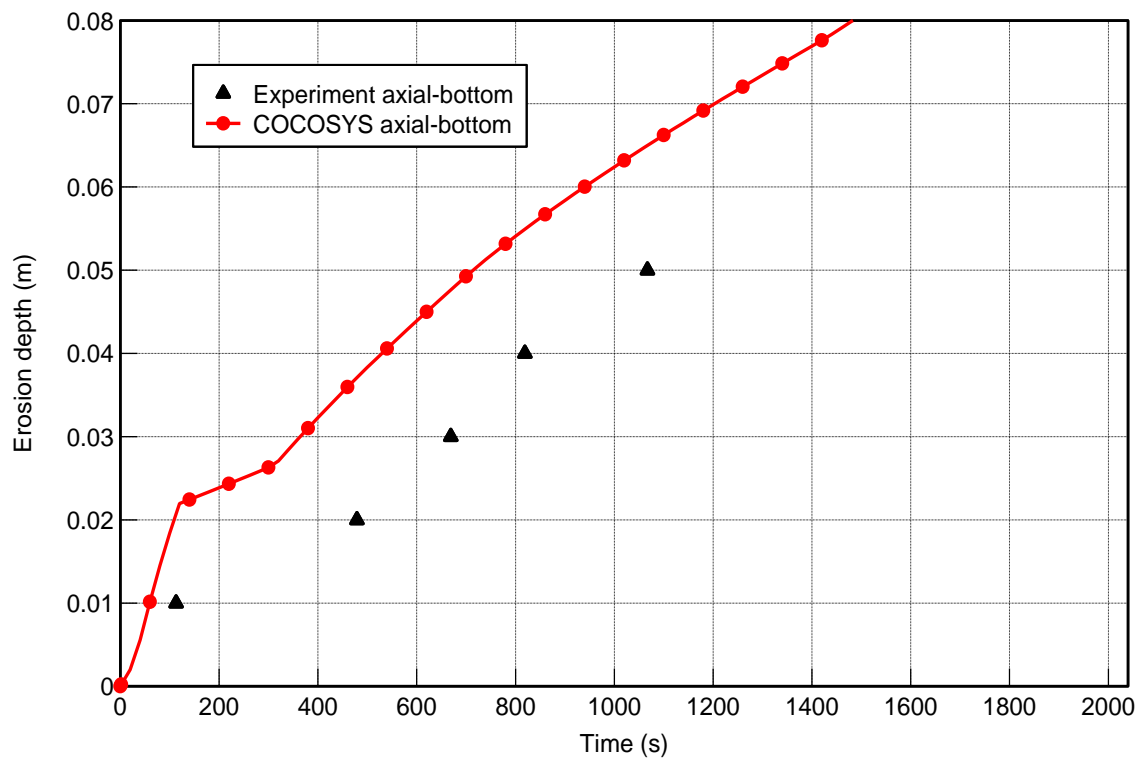


Fig. 2.20 MOCKA 5.7, axial ablation depth

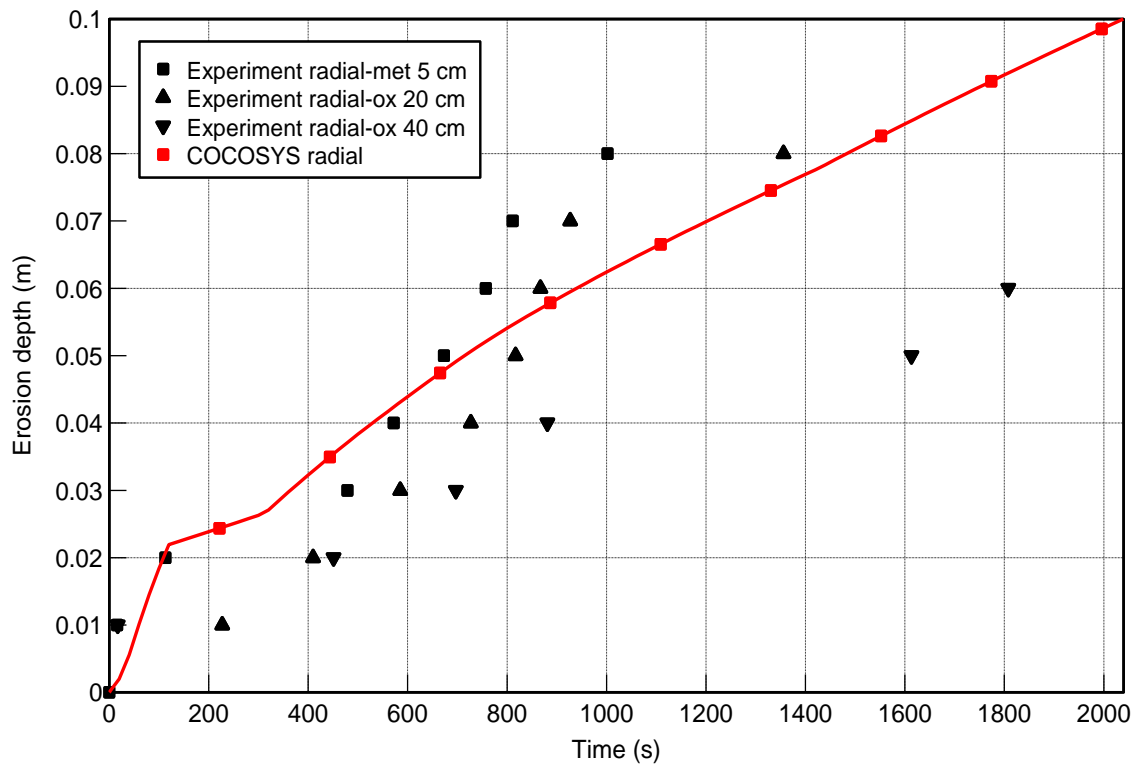


Fig. 2.21 MOCKA 5.7, radial ablation depth

On the other site, the measured temperatures relevant for the metal and oxide layers were used for the direct comparison with temperatures calculated by COCOSYS/CCI (Fig. 2.22). It should be remarked that the thermocouples are initially placed inside the concrete and give the information on the corium (melt mixture) temperature only after the corium is approaching to the couples.

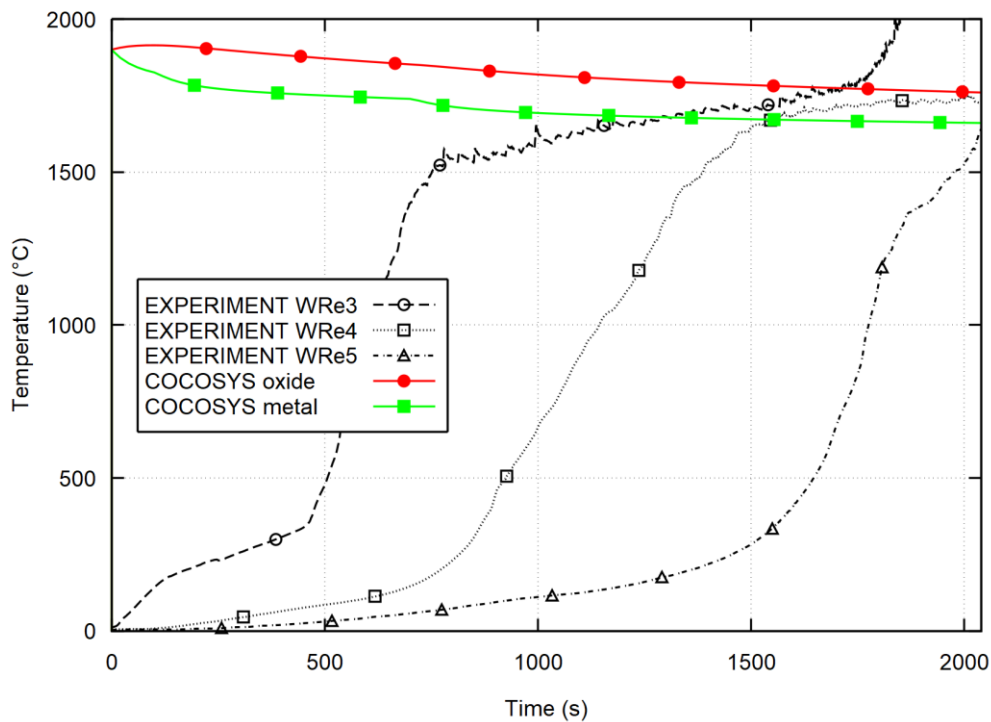


Fig. 2.22 MOCKA 5.7, oxide/metal phase temperature

2.2 Examples of plant application

In the following two examples of application for two different plants with full pressure containment are given: Konvoi and VVER-1000. For each plant selected results of an exemplary severe accident analysis with anticipated reactor pressure failure under certain initial and boundary conditions are demonstrated. For the Konvoi type plant a small break LOCA is analysed with focus on hydrogen behaviour, for the VVER-1000 plant a large break LOCA with focus on MCCI. It should be underlined that these results serve for demonstration of the code applicability, not for safety assessment.

2.2.1 Konvoi NPP

Konvoi is a German type NPP with PWR. In the early 1980th, the last three NPPs were built in Germany based on the same design and in quick succession. They are called Konvoi (convoy). This plant type has an electrical gross power of around 1400 MW. It is equipped with a double shell full pressure containment. The free volume under the inner spherical steel shell amounts to approximately 70000 m³. The equipment compartments are separated by rupture disc and flaps from the operating rooms of the containment.

2.2.1.1 Accident scenario

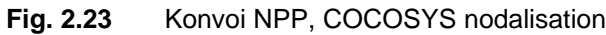
The exemplarily shown severe accident scenario represents a small break loss of coolant accident with the additional assumption that all active cooling systems fail. Thus, no heat removal system is operational, only the pressure accumulators inject water into the primary circuit. No feed water is injected into the steam generator either, leading to an failure of the reactor pressure vessel after 12280 s. Molten core concrete interaction leads to the melt trough of the biological shield after 49025 s. Consequently, the melt comes into contact with the sump water, leading to an increased steam production that significantly contributes to a strong pressure build-up in the containment.

2.2.1.2 COCOSYS model

In the COCOSYS model, the containment is represented by 279 zones, 920 junctions, and 554 structures. To simulate uplift of a light gas plume in the dome, plume zones (see zones D24A/C to D110 in Fig. 2.23) were situated in the dome starting at the top of the steam generator towers. The input deck was developed with a possible stratification in mind, the fine nodalisation of the great plant rooms (R65A/D-R67A/D), and the dome – starting from the steam generator towers (R20A/C, R21A/C) – (D23A/C-D110) makes a simulation of a stratification possible. Each steam generator tower has two zones per level to simulate a counter current flow, each of the rupture discs in their ceiling is split into a part connected to the plume (R21Ai/Ci to D24A/C) and into a part connected to the dome zone (R21Ao/Co to D23A/C). To avoid heat bridges via the annulus, for each zone inside the containment with direct contact to the steel shell one zone in the annulus is modelled.

To prevent possible hydrogen combustion 57 PARs are installed in different rooms and correspondingly considered in the model.

All necessary data regarding the accident progression in the primary circuit and the melt concrete interaction were simplified considered by means of tables for mass and energy injection of water, steam, H₂, CO, CO₂, and fission products.



The pressure behaviour of the atmosphere in the containment dome is given in Fig. 2.24. The first pressure rise in the containment up to reactor pressure vessel failure at around 12200 s is caused by the core heat-up followed by the core degradation influenced by the activation of the accumulators. After the failure of the pressure vessel and the core relocation to the dry cavity, the condensation of steam at the containment surfaces leads to a continuous pressure decrease in the containment. This trend is reversed at the time when the biological shield is assumed to fail after 49025 s. In the following phase, the contact of the melt with the sump water leads to a long-term pressure build-up in the containment that ultimately would trigger containment venting.

Fig. 2.26 shows exemplarily the gas composition (volume concentrations) of the atmosphere in the containment dome. The composition is dominated by the steam ratio leading to steam inertisation of the gas mixture already within the first hour after the start of the accident.

COCOSYS Short Description

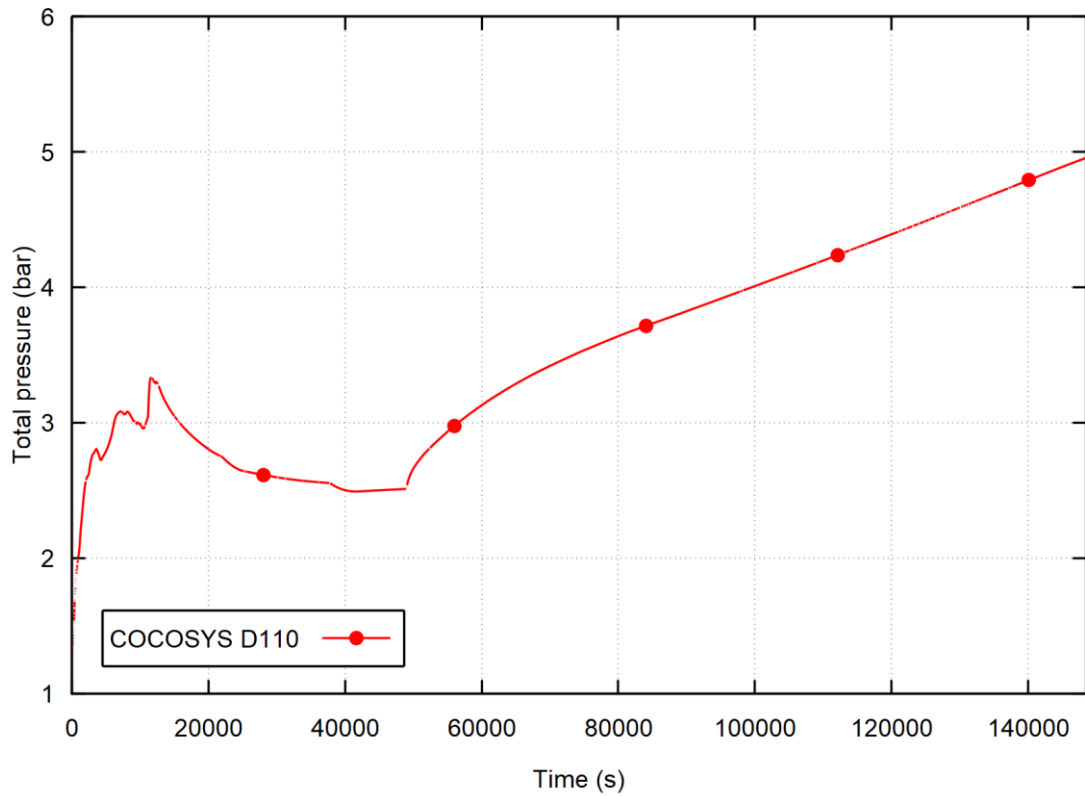


Fig. 2.24 Konvoi NPP, atmospheric pressure in containment dome

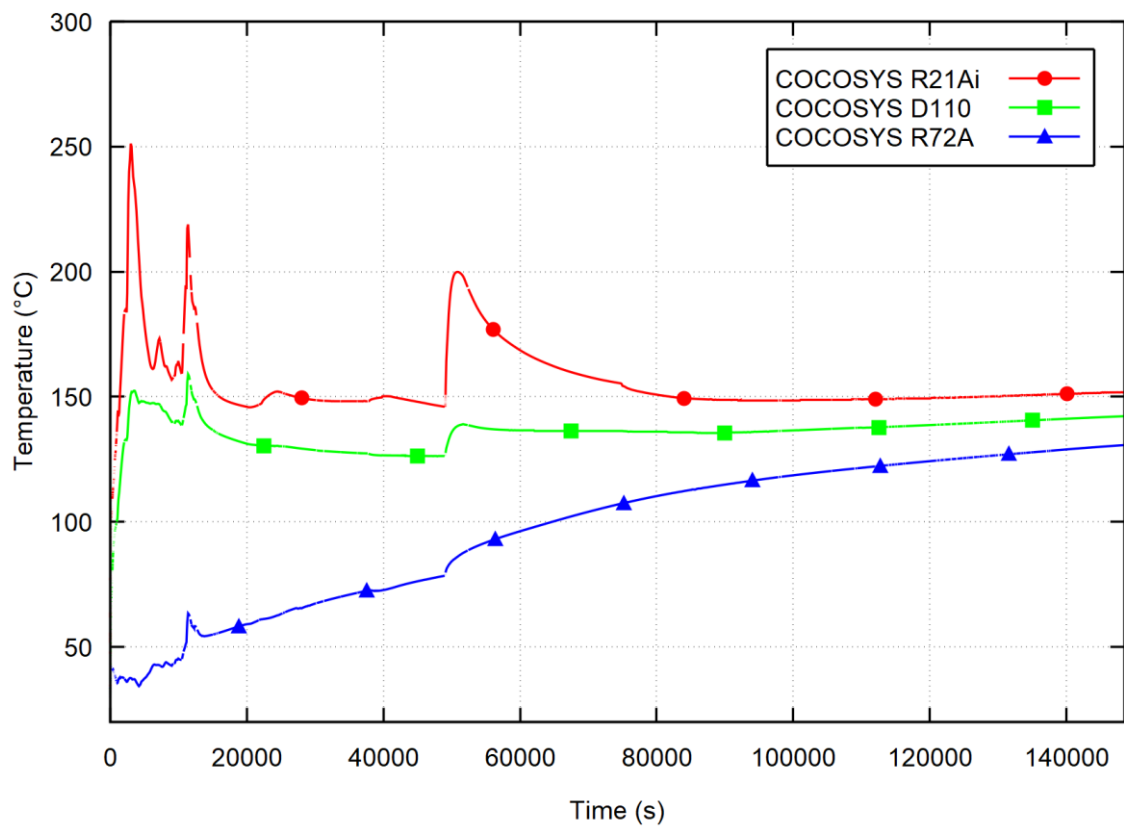


Fig. 2.25 Konvoi NPP, atmospheric temperature in selected containment zones

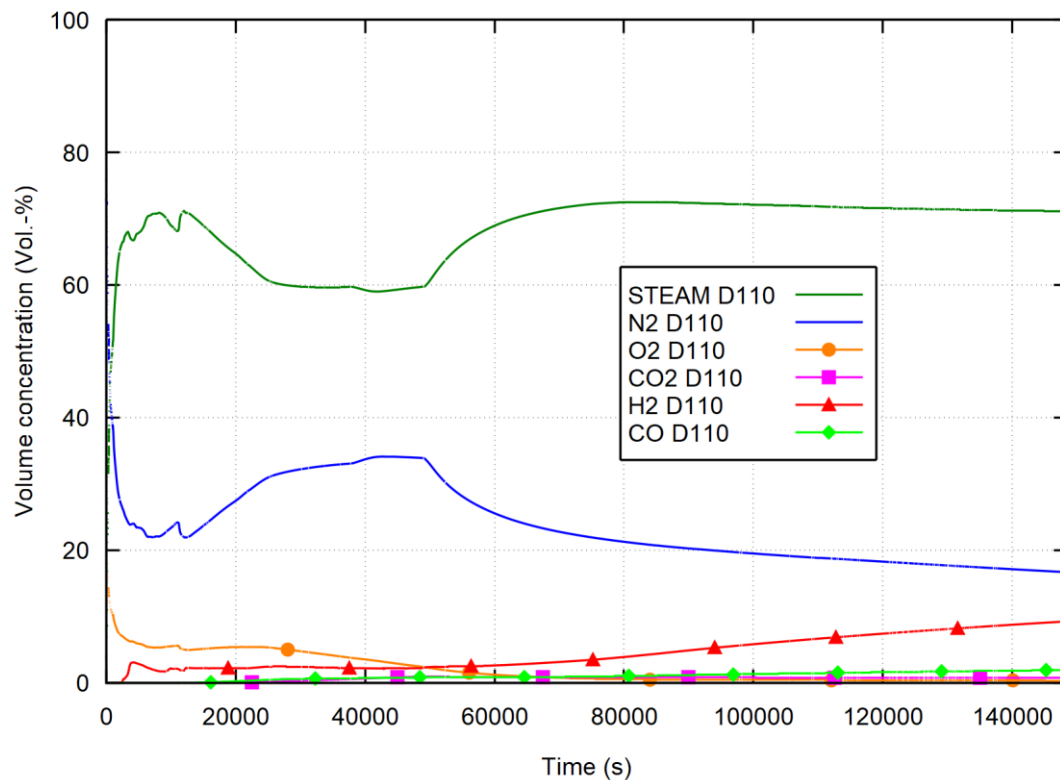


Fig. 2.26 Konvoi NPP, hydrogen concentration in uppermost dome zone D110

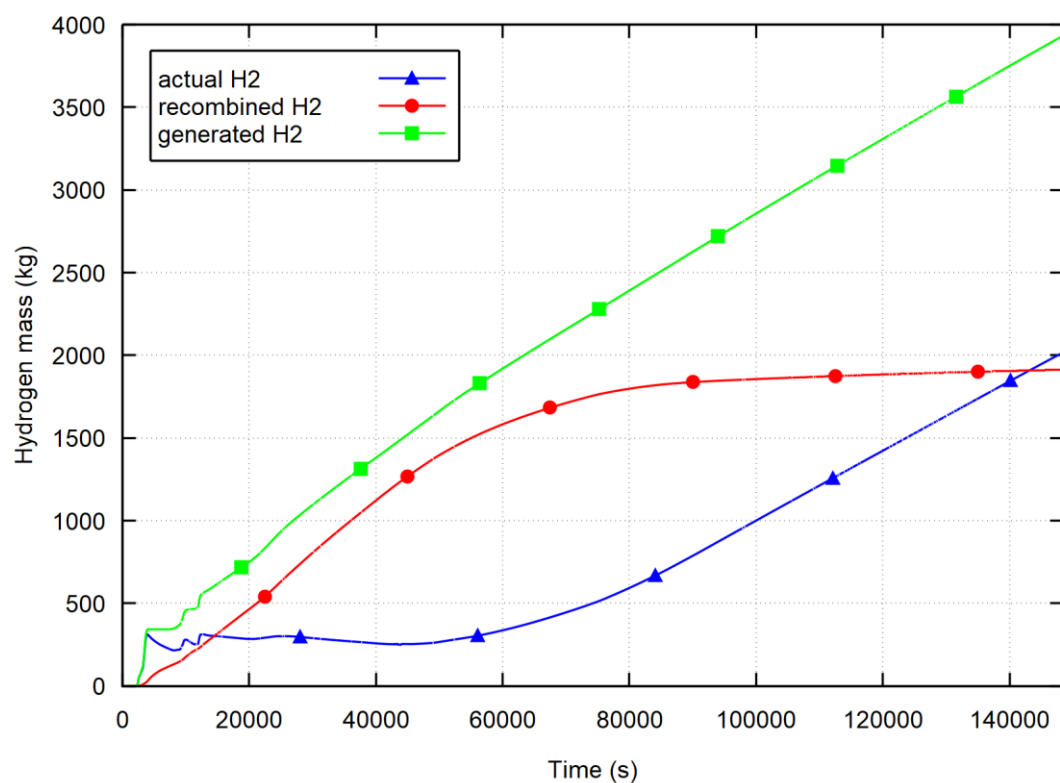


Fig. 2.27 Konvoi NPP, hydrogen mass in the containment

2.2.2 VVER-1000 NPP

VVER-1000 plants were originally developed in the former Soviet Union and are equipped with PWR. They have an electrical gross power of 1000 MW. The full pressure containment of VVER-1000/320 series consists of a single shell made of lined pre-stressed concrete. The free volume under the containment amounts to approximately 60000 m³.

2.2.2.1 Accident scenario

The exemplary COCOSYS results for the VVER-1000 application shown below were achieved for the anticipated severe accident scenario large break loss of coolant accident (LB LOCA) with simultaneous station blackout. Thus, no active core cooling system is available. Under the chosen boundaries the scenario is characterized by the reactor core heat-up, melting of the core and its drop to the reactor's lower head, and the lower head failure at 11700 s after start of the accident. Shortly after this, the corium comes into contact with the sump water in the reactor cavity, leading to a heavy steam generation, followed by a strong pressure build-up in the containment.

2.2.2.2 COCOSYS model

The COCOSYS model developed for the investigation of severe accidents including MCCI comprises 95 zones, 184 atmospheric and 97 drain junctions, and 326 heat structures. Its nodalisation is shown in Fig. 2.28. It was developed with focus on the plant long-term response including processes during MCCI calculated with the CCI module under assumptions in correspondence with the state-of-the-art conditions.

2.2.2.3 Selected results

Fig. 2.29 shows the calculated atmospheric pressure in the break zone and in the uppermost region of the containment dome of a VVER-1000 NPP during the anticipated severe LB LOCA scenario. The first comparatively short pressure rise in the containment compartments is caused by the high energetic release of steam and water through the large break into the containment atmosphere. Injection from the hydro-accumulators cools down the reactor temporarily and together with steam condensation at the containment walls leads to depressurisation of the containment until the reactor pressure vessel failure at 11700 s. Immediately from this time on until about 24000 s, pressure and temperature of the containment atmosphere (Fig. 2.30) increase steadily caused by the heavy steam generation as result of the contact between the corium and the water in the reactor cavity. After drying out of the cavity the containment compartments are pressurised by the hot non-condensable gases released during the MCCI. At the end of this exemplary calculation the pressure approaches to a pressure level requiring venting of the containment, which not modelled in this exemplary calculation.

The axial and radial erosion depths calculated with the CCI module of COCOSYS for the reactor cavity (see zone c-8_2 in Fig. 2.28) is depicted in Fig. 2.31. Used CCI model parameters (e.g. heat transfer coefficients between corium and concrete) and given geometrical characteristics lead to the uniformity of the calculated average erosion depths.

Fig. 2.32 shows the resulting temperature of the corium mixture in the reactor cavity. After about 18000 s, Zr and Cr in the corium mixture are fully oxidized. Thus, the energy released by the MCCI reactions is reduced which leads to a slight decrease of the corium temperature. During the whole calculated process time in the ex-vessel phase, the corium temperature remains above the decomposition temperature of the basemat concrete.

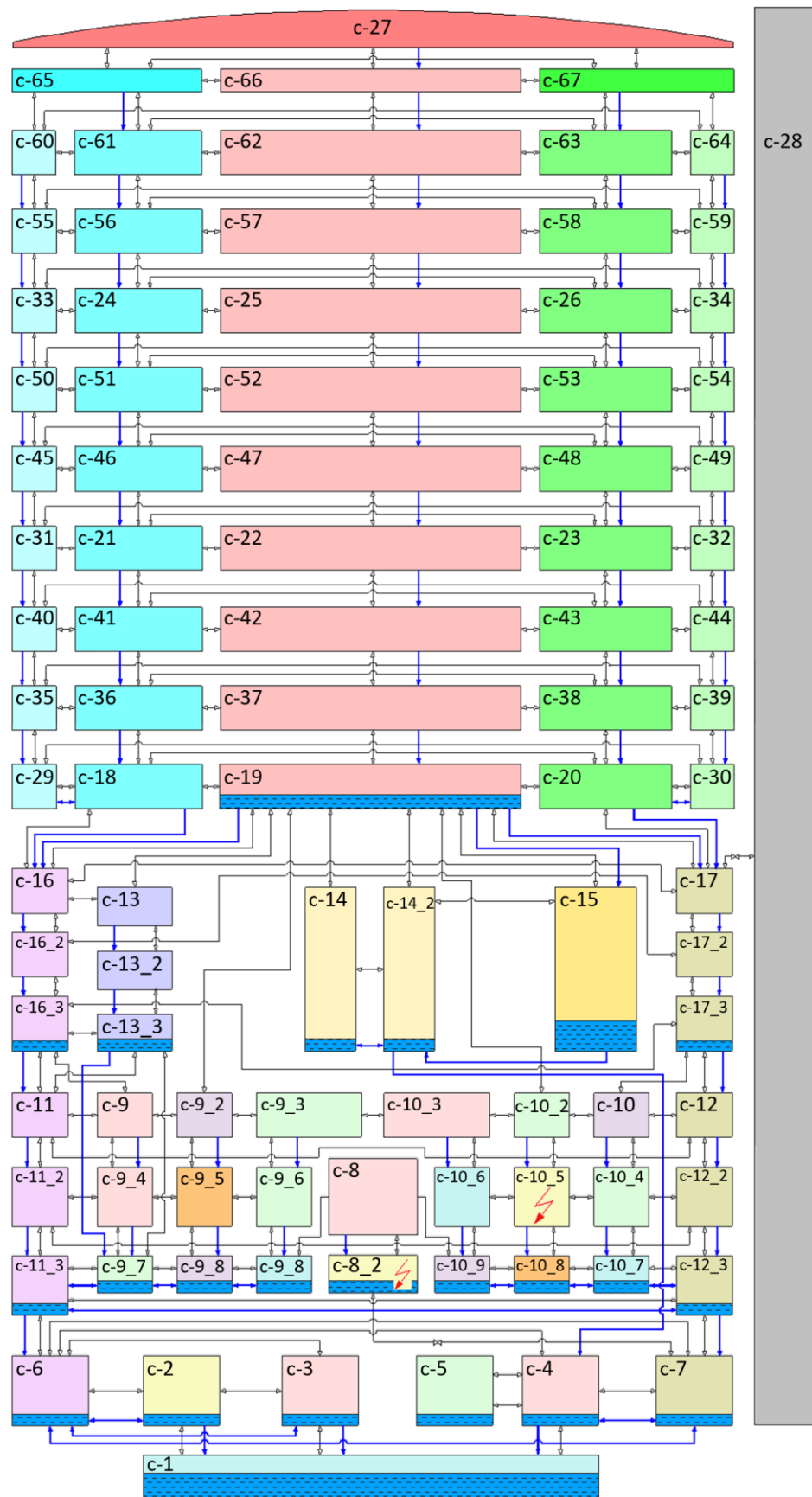


Fig. 2.28 VVER-1000 NPP, COCOSYS nodalisation with 95 zones

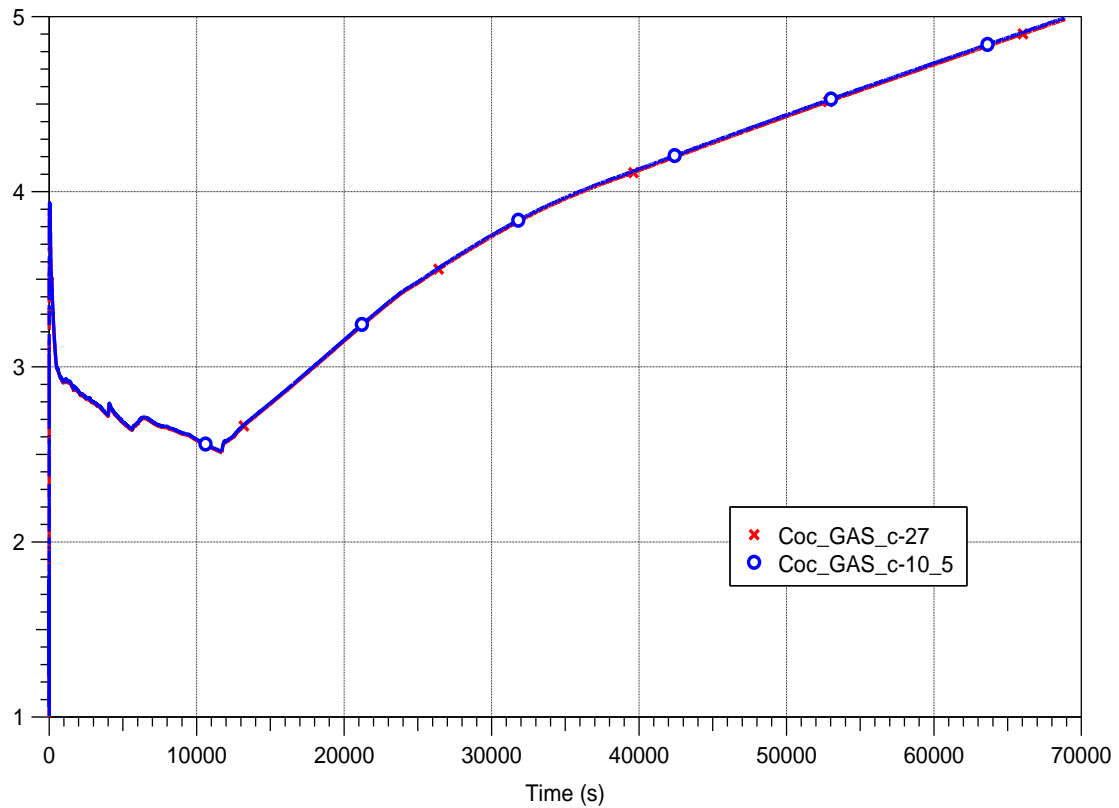


Fig. 2.29 VVER-1000 NPP, atmospheric pressure in containment dome and break zone

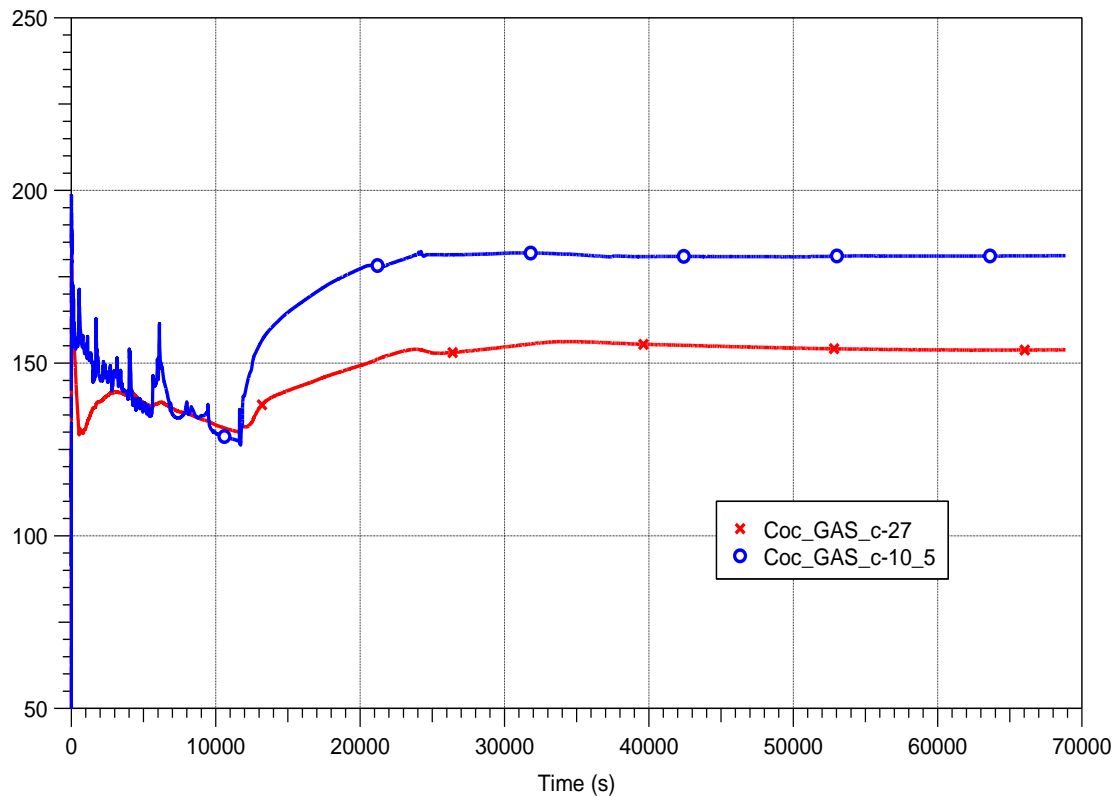


Fig. 2.30 VVER-1000 NPP, atmospheric temperature in containment dome and break zone

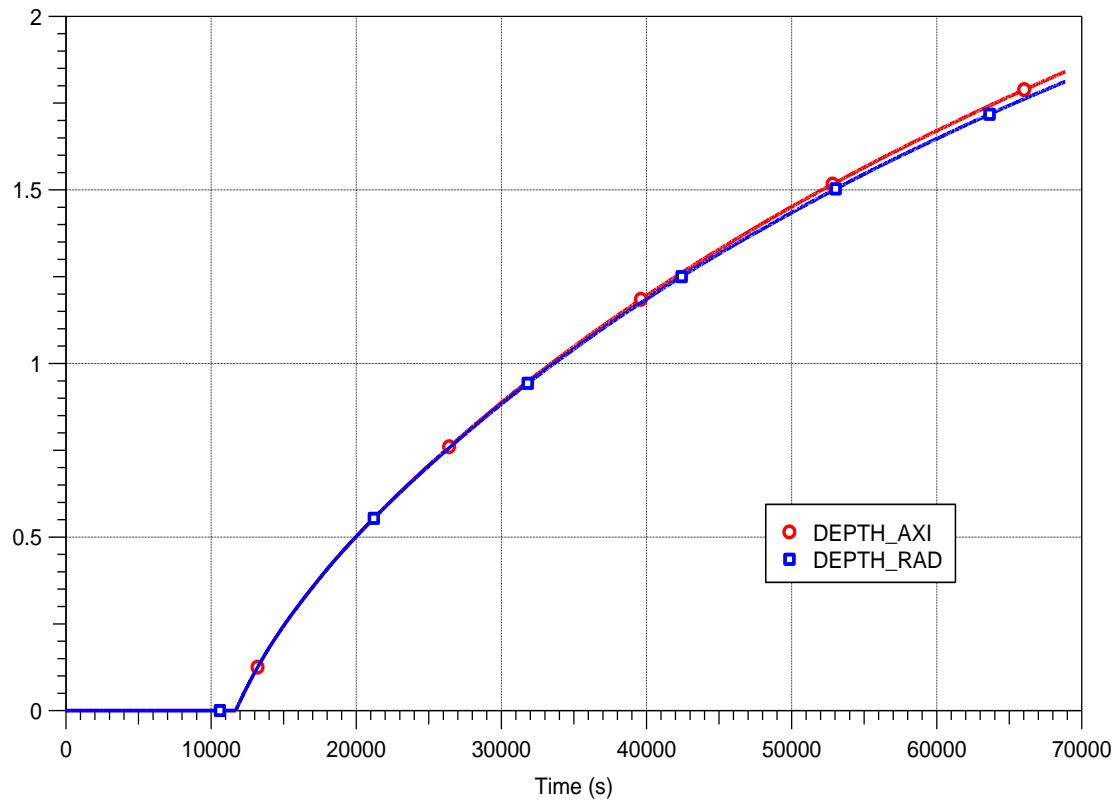


Fig. 2.31 VVER-1000 NPP, axial and radial concrete erosion depths

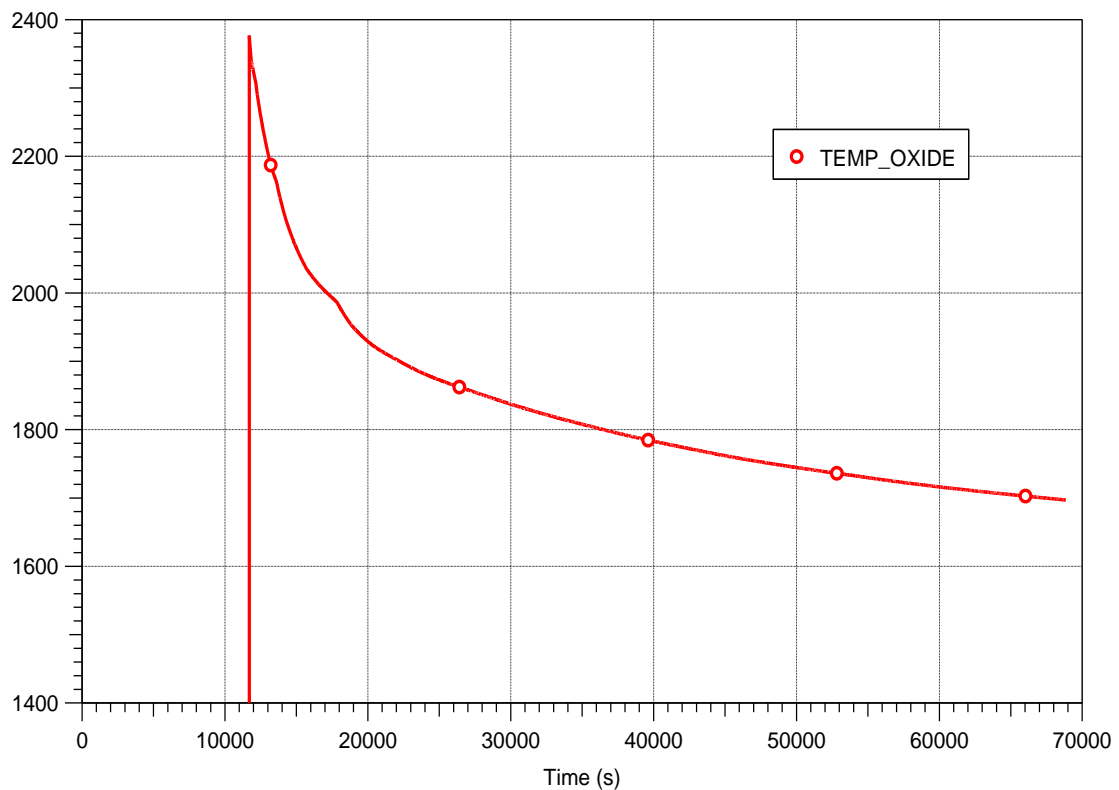


Fig. 2.32 VVER-1000 NPP, temperature of corium mixture in the reactor cavity

3 References

- /ARN 98/ Arndt, S., Weber, G.: FIPHOST - A Module to Calculate the Fission Product Transport in a LWR Containment. Gesellschaft für Anlagen- und Reaktorsicherheit (GRS) gGmbH, GRS-A-2553, 93 S.: Köln, 1998.
- /ARN 19/ Arndt, S., Band, S., Beck, S., Eschricht, D., Iliev, D., Klein-Heßling, W., Nowack, H., Reinke, N., Sonnenkalb, M., Spengler, C., Weber, G., Brückner, N.: COCOSYS_3.0.1_User_Manual. Hrsg.: GRS gGmbH, 983 S., 2019.
- /BAR 07/ Barrachin, M., Cousin, F.: MDB : a Databank of Material Properties for Water Cooled Reactors. Hrsg.: IRSN, ASTEC Documentation, DPAM/SEMIC-2007/311, 594 S.: Saint-Paul-lez-Durance Cedex France, 2007.
- /BEC 20/ Becker Technologies GmbH: THAI-Facility & Program. Stand vom 21. September 2020, erreichbar unter <https://www.becker-technologies.com/pdf/thai.pdf>, abgerufen am 21. September 2020.
- /CRA 05/ Cranga, M., Fabianelli, R., Jacq, F., Barrachin, M., Duval, F.: The MEDICIS code, a versatile tool for MCCI modelling. In: American Nuclear Society (Hrsg.): International Congress on Advances in Nuclear Power Plants 2005. Seoul, 15. - 19. Mai 2005, 2005.
- /FIS 98/ Fischer, K.: Modellierung von Abscheidungsverfahren in Wasservorlagen: Abschlussbericht. Battelle Ingenieurtechnik GmbH, BF-R68.411-1, 1998.
- /FOI 19/ Foit, J. J., Cron, T., Fluhrer, B.: Melt/Concrete Interface Temperature Relevant to MCCI Process. In: ÚJV Řež: ERMSAR2019, The 9th European Review Meeting on Severe Accident Research. ERMSAR 2019, Prague, Czech Republic, 18. - 20. März 2019, 2019.
- /HES 98/ Hesse, U.: FIPIISO-98 ein Rechenmodell zum Nuklidverhalten in einem Raumzellensystem nach einem Reaktorstörfall. Gesellschaft für Anlagen- und Reaktorsicherheit (GRS) gGmbH, GRS-A-2750: Köln, 1998.
- /INT 20/ Intel Corp.: Intel MPI. Erreichbar unter <https://software.intel.com/en-us/mpi-library>, abgerufen am 28. August 2020.
- /ISA 19/ Isaakson, P., et al.: Corium interaction with basaltic concrete (typical for Nordic LWRs) with and without rebars. Hrsg.: SAFEST-DRI-D3.2.6, 2019.
- /KÓS 07/ Kóska, P.: Development and Assessment of Fission Product Release Model for MEDICIS (ASTEC). Hrsg.: Institute for Electric Power Research Co., VEIKI Institute for Electric Power Research Co., VEIKI 21.51-726, 31 S.: Budapest, Dezember 2007.
- /LUT 96/ Luther, W., Romstedt, P.: Verbesserung der Zeitintegration und des Sparse Matrix Pakets in ATHLET. GRS, GRS-A-, Nr. 2356, Mai 1996.
- /MEL 03/ Melikhov, O., Osokin, G.: Two SLB Tests at BC V-213 Test Facility, Quick Look Report. EREC Electrogorsk, February / 2003.

- /SPE 01/ Spengler, C.: LAVA 2000, A computer code for the simulation of melt spreading in the containment; [program description]. GRS-A-, Bd. 2968, 1. Aufl., XII, 85 S, GRS: Köln, 2001.
- /WEB 09/ Weber, G., Funke, F.: Description of the Iodine Model AIM-3 in COCOSYS. Hrsg.: GRS gGmbH, GRS-A-, Nr. 3508, 100 S.: Garching b. München, November 2009.
- /ZEM 19/ Zemitis, A., Iliev, O., Steiner, K.: CoPool - User's Manual, Code revision 1218. Fraunhofer ITWM, February / 2019.